



Published in final edited form as:

Mol Cell. 2019 February 21; 73(4): 845–856.e5. doi:10.1016/j.molcel.2018.12.022.

ELTA: Enzymatic Labeling of Terminal ADP-ribose

Yoshinari Ando^{1,2}, Elad Elkayam^{2,3}, Robert Lyle McPherson^{1,2}, Morgan Dasovich^{1,4}, Shang-Jung Cheng^{1,4}, Jim Voorneveld⁵, Dmitri V. Filippov⁵, Shao-En Ong⁶, Leemor Joshua-Tor³, and Anthony K. L. Leung^{1,7,8,*}

¹Department of Biochemistry and Molecular Biology, Bloomberg School of Public Health, Johns Hopkins University, Baltimore, MD 21205, USA ²These authors contributed equally ³Keck Structural Biology Laboratory, Howard Hughes Medical Institute, Cold Spring Harbor Laboratory, Cold Spring Harbor, NY 11724, USA ⁴These authors contributed equally ⁵Gorlaeus Laboratories, Leiden Institute of Chemistry, Leiden University, Einsteinweg 55, 2333 CC Leiden, The Netherlands ⁶Department of Pharmacology, University of Washington, Seattle, WA 98195, USA ⁷Department of Molecular Biology and Genetics, School of Medicine, Johns Hopkins University, Baltimore, MD 21205, USA ⁸Department of Oncology, School of Medicine, Johns Hopkins University, Baltimore, MD 21205, USA

SUMMARY

ADP-ribosylation refers to the addition of one or more ADP-ribose groups onto proteins. The attached ADP-ribose monomers or polymers, commonly known as poly(ADP-ribose) (PAR), modulate the activities of the modified substrates or their binding affinities to other proteins. However, progress in this area is hindered by a lack of tools to investigate this protein modification. Here, we describe a new method named ELTA (**E**nzymatic **L**abeling of **T**erminal **A**D**P**-ribose) for labeling free or protein-conjugated ADP-ribose monomers and polymers at their 2'-OH termini using the enzyme OAS1 and dATP. When coupled with various dATP analogs (e.g., radioactive, fluorescent, affinity tags), ELTA can be used to explore PAR biology with techniques routinely used to investigate DNA/RNA function. We demonstrate that ELTA enables the biophysical measurements of protein binding to PAR of a defined length, detection of PAR length from proteins and cells, and enrichment of sub-femtomole amounts of ADP-ribosylated peptides from cell lysates.

Graphical Abstract

*Corresponding Author and Lead Contact. Correspondence should be addressed to A.K.L.L. (anthony.leung@jhu.edu).

AUTHOR CONTRIBUTIONS

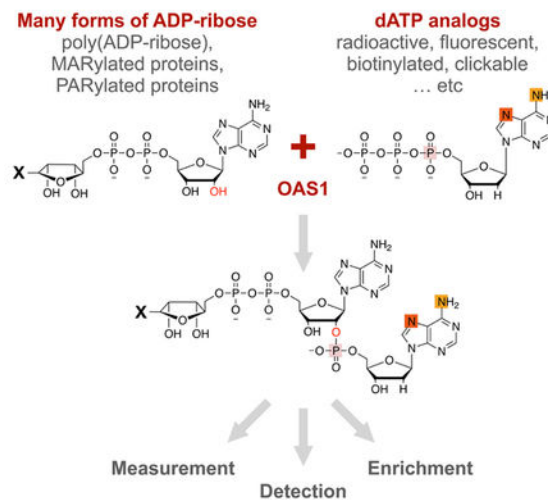
Conceptualization, A.K.L.L.; Methodology, Y.A., E.E., R.L.M., and A.K.L.L.; Investigation, Y.A., E.E., R.L.M., M.D., S-J.C., S-E.O., and A.K.L.L.; Resources, J.V., and D.F.; Writing – Original Draft, Y.A., E.E., R.L.M., and A.K.L.L.; Writing – Review & Editing, Y.A., E.E., R.L.M., M.D., S-J.C., D.V.F, S-E.O., L.J-T, and A.K.L.L.; Supervision, D.F., S-E.O., L.J-T, and A.K.L.L.; Funding Acquisition, R.L.M., S-E.O., L.J-T, and A.K.L.L.

Publisher's Disclaimer: This is a PDF file of an unedited manuscript that has been accepted for publication. As a service to our customers we are providing this early version of the manuscript. The manuscript will undergo copyediting, typesetting, and review of the resulting proof before it is published in its final citable form. Please note that during the production process errors may be discovered which could affect the content, and all legal disclaimers that apply to the journal pertain.

DECLARATION OF INTERESTS

A patent on the ELTA technique was provisionally filed on April 2nd, 2018.

ELTA: Enzymatic Labeling of Terminal ADP-ribose



Abstract

Ando, Elkayam and McPherson et al describe a simple, efficient and versatile platform technology called ELTA to label free or protein-conjugated ADP-ribose monomers and polymers with dATP analogs (radioactive, fluorescent, biotin, clickable tags, etc). With these functionalized tags, ELTA simplifies the measurement, detection and enrichment of various forms of ADP-ribose.

INTRODUCTION

ADP-ribosylation involves the transfer of ADP-ribose from NAD⁺ onto proteins post-translationally in unicellular and multicellular organisms (Gupte et al., 2017; Palazzo et al., 2017). ADP-ribose can be added singly as mono(ADP-ribose) (MAR) or in polymeric form as poly(ADP-ribose) (PAR) by ADP-ribosyltransferases, including a family of enzymes commonly known as poly(ADP-ribose) polymerases (PARPs) (Cohen and Chang, 2018; Hottiger et al., 2010; Lüscher et al., 2018; Palazzo et al., 2017; Pascal and Ellenberger, 2015). ADP-ribosylation can be reversed by macrodomain-containing enzymes, including poly(ADP-ribose) glycohydrolase (PARG) (Barkauskaite et al., 2013; Feijs et al., 2013; Pascal and Ellenberger, 2015). The delicate balance of ADP-ribosylation is critical for regulating DNA damage repair, transcription, chromatin structure, non-membranous structure formation, host-pathogen interactions and RNA metabolism (Bock et al., 2015; Hottiger, 2015; Leung, 2014; Lüscher et al., 2018; Zhen and Yu, 2018). Dysregulation of ADP-ribosylation or PARP activity has been implicated in the pathogenesis of diseases including cancers, virus infection and neurodegeneration (Lüscher et al., 2018; Rouleau et al., 2010). Inhibitors of certain PARP family members have already shown promise in treating ovarian, prostate, breast and other cancers, with three drugs approved by the FDA (Lord and Ashworth, 2017). Additionally, these inhibitors could be repurposed for non-oncological diseases (Berger et al., 2017). Though this therapeutically important modification was discovered in 1963, the progress in understanding its structure, interaction, and biology has been hampered by a lack of tools.

Apart from being a protein modification, PAR is a polynucleotide that is chemically similar to DNA or RNA. The measurement, detection and enrichment of DNA/RNA *in vitro* and from cells have been made possible by the rather straightforward modification of these nucleic acids with a variety of useful tags (e.g., fluorophores, radioactive or biotin) at either terminus using enzymes. The lack of a similar bioconjugation technology for PAR makes it difficult to adapt existing molecular biology techniques to investigate this polynucleotide.

DESIGN

ADP-ribose has two ribose moieties: one as part of an adenosine group and a non-adenosine ribose that exists in an equilibrium between a closed, dominant form and an open chain form, which possesses an aldehyde group at its 1'' position (Fig. S1a, green). The 1'' position is chemically reactive and can be conjugated to either a protein or to another ADP-ribose from NAD⁺ to form PAR. It has previously been shown that this 1'' aldehyde group can also be used for end-labeling through chemical conjugation to carbonyl-reactive biotin analogs with 10–20% efficiency (Fahrer et al., 2007). As such, this 1'' aldehyde group is unavailable for labeling when ADP-ribose is conjugated to a protein. Here we describe a new method named ELTA (Enzymatic Labeling of Terminal ADP-ribose) to label free or protein-conjugated ADP-ribose monomers and polymers at their 2'-OH termini. We demonstrate that ELTA is a sensitive approach to label and assess the length of PAR isolated from proteins and cells. When coupled with different chemical analogs, ELTA can be used for various applications including fluorescence-based biophysical measurement of PAR-protein interaction and enrichment of ADP-ribosylated peptides for mass spectrometry identification.

To label ADP-ribose and its derivatives at the 2'-OH terminus (Fig. 1a and S1a, red), we used the double-stranded RNA-activated human enzyme 2'-5'-Oligoadenylate Synthetase 1 (OAS1) (Hornung et al., 2014; Justesen et al., 2000; Kristiansen et al., 2011). OAS1 oligomerizes ATP into 2'-5' linked oligoadenylate, where the α -phosphate of the donor ATP is linked to the 2'-OH of the acceptor ATP and the resultant AMP moiety with a free 2'-OH serves as an additional acceptor to facilitate oligomerization (Hornung et al., 2014; Justesen et al., 2000; Kristiansen et al., 2011). Two pieces of data suggested that OAS1 would have the potential to be used as a labeling tool for ADP-ribose. First, apart from ATP, OAS1 can use other derivatives of adenosine with free 2'-OH group as acceptors, including NAD⁺ (Ball and White, 1979; Ferbus et al., 1981) and ADP-ribose (Cayley and Kerr, 1982). Second, OAS1 can use other NTPs such as deoxy-ATP (dATP) (Justesen et al., 2000) as donors. Because dATP lacks a 2'-OH group and it cannot serve as an OAS1 acceptor for further chain extension (Justesen et al., 1980), we reason that it will be useful for end-labeling. Therefore, if dATP could be added to the 2'-OH terminus of free and protein-conjugated ADP-ribose monomers or polymers, dATP would be an ideal donor substrate of OAS1 to end-label these types of acceptor molecules.

RESULTS

The basis of ELTA: Enzymatic addition of dAMP onto 2'-OH termini of ADP-ribose monomers and polymers by OAS1

To test whether OAS1 can use dATP as a donor substrate for ADP-ribose in vitro, recombinant OAS1 activated by poly(I:C) dsRNA was incubated with ADP-ribose and α - ^{32}P -dATP (hereafter ^{32}P -dATP). In agreement with our premise, a major radioactive product running above ^{32}P -dATP was observed (Fig. 1b, S1b). Similarly, OAS1 labels NAD^+ , but not the *iso*-ADP-ribose (the internal unit of PAR which has the same chemical composition as ADP-ribose) presumably because the latter lacks an adenosine moiety with a free 2'-OH (Fig. S1b). To further confirm the addition of a dAMP moiety onto ADP-ribose by OAS1, we used matrix assisted laser desorption ionization-time of flight (MALDI-TOF) mass spectrometry analysis to monitor an in vitro labeling experiment of ADP-ribose and dATP in 1:1 ratio (Fig. 1c). In the absence of OAS1, dATP and ADP-ribose were observed at m/z of 492.0 and 560.0, respectively. In the presence of OAS1, the peaks for ADP-ribose and dATP were significantly reduced with an additional peak observed at m/z of 873.0, corresponding to the expected $[\text{M}+\text{H}]^+$ of ADP-ribose-dAMP product.

Given that the internal unit of PAR cannot be labeled (Fig. S1b) but each linear PAR chain has one 2'-OH terminus (Fig. S1a), we next investigated whether different lengths of PAR can also be end-labeled. Short (15-mer), medium (15–40-mer) and long (40-mer) PAR polymers (Tan et al., 2012) were incubated with OAS1 and ^{32}P -dATP (Fig. 1b). In each case, these PAR molecules of different lengths were effectively labeled (Fig. 1b). To test whether PAR length affects labeling efficiency, we optimized a purification method (Tan et al., 2012) to efficiently separate PAR into defined chain lengths (Fig. S1c). We then used the same ^{32}P -dATP/OAS1 method to label equal amounts of defined PAR length chains (Fig. S1d). As expected, PAR chains of different lengths were labeled with comparable efficiency (Fig. S1d). Taken together, OAS1 can label both ADP-ribose monomers and polymers using radiolabeled dATP.

OAS1 adds dAMP onto protein-conjugated ADP-ribose

As ADP-ribose can be covalently linked to a protein at its 1' terminus (Fig. S1a), we reasoned that a protein-conjugated ADP-ribose with a free 2'-OH group could also be served as an OAS1 substrate. Using either automodified PARP10 catalytic domain (PARP10^{CD}) (Kleine et al., 2008) or *Herpetosiphon aurantiacus* PARP (*ha*PARP) (Slade et al., 2011) as model substrates, respectively, for mono(ADP-ribosyl)ated (MARylated) and poly(ADP-ribosyl)ated (PARylated) proteins, we tested whether these ADP-ribosylated substrates can be labeled by OAS1 with ^{32}P -dATP (Fig. 1d, e). As a negative control, we pre-treated the ADP-ribosylated substrates with *hs*NudT16 (Daniels et al., 2015b; Palazzo et al., 2015), which cleaves the pyrophosphate bond within ADP-ribose (cf. Fig. S1a) to leave a phosphoribose group on protein residues that were previously ADP-ribosylated. As a result, the 2'-OH containing adenosine-linked ribose is removed, and these phosphoribosylated proteins are no longer recognized by the Afl521 macrodomain (pan-ADP-ribose reagent; Gibson et al., 2017) nor are substrates for OAS1 labeling (Fig. 1d, e). On the other hand, MARylated PARP10^{CD} and PARylated *ha*PARP were indeed labeled by ^{32}P -dATP in the

presence of OAS1 (Fig. 1d, e). Therefore, this OAS1-based method presents a novel approach to label both protein-conjugated ADP-ribose monomers and polymers.

OAS1 is a versatile enzyme that accepts different modified dATP analogs for labeling

Next, we investigated whether the OAS1 enzymatic labeling reaction can be extended to the labeling of ADP-ribose with modified dATP analogs. Following a similar labeling protocol, we used Cy5-dATP attached at two different positions on the adenine base (N6 and N7; Fig. 1a and S2a). We efficiently labeled three different PAR chain lengths (10-mer, 15-mer, and 20-mer) and a mixture of 6–23-mer PAR chains with the two Cy5 analogs (Fig. S2a). PAR is completely labeled when Cy5-dATP is used in five-fold excess or more (Fig. S2b–c). OAS1 labeling can also be performed with other fluorescent derivatives such as Cy3 (Fig. S2d), or with biotinylated dATP (Fig. S2e). In addition, this labeling reaction can also be performed on protein-conjugated ADP-ribose using modified dATP as well as performed in a range of detergent and denaturing conditions (Fig. S1e and S2f–i).

Given the versatility of OAS1 to label free and protein-conjugated ADP-ribose using a range of dATP analogs (Fig. 1a), we present this approach as a general method to enzymatically label terminal ADP-ribose and named it ELTA (**E**nzymatic **L**abeling of **T**erminal **A**DP-ribose). Using several proof-of-concept applications, we illustrate how to use ELTA for measurement (Fig. 2), detection (Fig. 3) and enrichment (Fig. 4) while investigating ADP-ribosylation biology.

Labeled PAR chains can be used to measure the affinity of PAR binding to proteins in vitro

PARylation of target proteins regulates many biological processes (Gupte et al., 2017; Hottiger, 2015; Leung, 2014; Lüscher et al., 2018; Palazzo et al., 2017). For example, PAR recognition by the WWE domain of RNF146 is required for the poly-ubiquitination and subsequent degradation of axin—a key regulator of the *Wnt* signaling pathway (Zhang et al., 2011). PAR-binding affinity has been previously assayed using fluorescently labeled di-ADP-ribose by fluorescent polarization (Lambrecht et al., 2015), or biotinylated PAR by electrophoretic mobility shift assay or surface plasmon resonance (Fahrer et al., 2007; 2010). However, both methods require PAR synthesis and conjugation through chemical approaches to label the PAR, which are not readily accessible to most molecular biology laboratories. Alternatively, PAR-binding affinity can be assayed with either a mixed population of PAR or with the internal unit *iso*-ADP-ribose as a proxy (Wang et al., 2012; Zhang et al., 2014) using isothermal titration calorimetry (ITC), which requires significant amounts of materials (typically at M concentrations). By combining ELTA with our improved single-length PAR chain purification (Fig. 2a and Fig. S1c), we were able to measure the affinity of a single-length PAR chain to the WWE domain of RNF146. First, we used a filter-binding assay and measured the affinity of radiolabeled 10- and 20-mer PAR to the RNF146 WWE domain (Fig. 2b). Both PAR chains bind tightly to the RNF146 WWE domain with binding constants of 75 ± 2.5 nM (10-mer) and 67 ± 2.3 nM (20-mer). We further extended our repertoire of biophysical measurements of the PAR binding assays by using the commonly used Cy5 fluorescence dye and measured the affinity of Cy5-PAR to the RNF146 WWE domain (100 ± 9 nM; Fig. 2c) using Microscale Thermophoresis (MST) (Wienken et al., 2010). Binding constants from both methods are similar considering the use of different

methodologies. However, when compared to the affinity reported for RNF146 WWE domain binding to *iso*-ADP-ribose that was used by Wang et al. 2012 and Zhang et al., 2014, a small but noticeable difference was observed (67–100nM compared to 180–370nM; Wang et al., 2012; Zhang et al., 2014). These differences could be readily explained by the different sizes of the ligands used—the full polymer vs. the internal unit *iso*-ADP-ribose as a proxy—where a longer PAR chain that harbors a high net negative charge would be expected to bind with higher affinity. Indeed, the binding constant obtained using ITC of another PAR binding protein, hSSB1, titrated with a mixture of 10–25-mer PAR ($K_d=150$ nM, Zhang et al., 2014) yielded a similar binding constant to those observed in our study.

Detection of polymer length of PAR isolated from individual proteins and cells

The number of ADP-ribose units attached to proteins is dynamically regulated within cells and, notably, protein binding to PAR is dependent on its chain length in some cases (Fahrer et al., 2007; Leung, 2014; Min et al., 2013; Popp et al., 2013). Though it is possible to visualize the length of PAR polymers using SYBR Gold or silver stain (Malanga et al., 1995), such methods cannot be used to visualize very short polymers (Fig. S1d and S3a). Alternatively, it is possible to infer the length of PAR from ADP-ribosylated proteins only if they are modified with radioactive NAD^+ in vitro. Given that ELTA can effectively add a single label to each 2'-OH terminus of pre-made PAR, we tested whether this labeling technique can be used to determine the chain length of PAR isolated from proteins already ADP-ribosylated and compare with the existing technique that requires radioactive NAD^+ incorporation. To examine the labeling efficiency of PAR isolated from PARylated PARP1, we performed automodification of PARP1 with 1 mM NAD^+ with or without a trace of ^{32}P - NAD^+ for either 0, 10, or 30 min (Fig. 3a). The non-radioactive protein samples were, on the other hand, labeled by OAS1 with ^{32}P -dATP (no unlabeled dATP). PAR was then extracted from both ^{32}P - NAD^+ and ^{32}P -dATP labeled samples and visualized by autoradiography. PAR isolated from ADP-ribosylated proteins can be efficiently labeled and the patterns of isolated PAR samples labeled by ^{32}P - NAD^+ and ^{32}P -dATP are comparable in length distribution (Fig. 3a). We note that the commercially available ^{32}P - NAD^+ is limited at ~ 7 μM , which is insufficient for most in vitro modification without the addition of unlabeled NAD^+ and thereby constitutes only a small fraction of ADP-ribose incorporated ($<0.003\%$ in this case). In contrast, the ^{32}P -dATP signal directly reflects the number of 2'-OH termini of PAR labeled by OAS1. To further illustrate the potential of the use of ELTA in assessing PAR length of ADP-ribosylated proteins/complexes, we modified PARP1 with NAD^+ in the absence or presence of its interacting protein HPF1. HPF1 binding alters PARP1 substrate specificity by reducing auto-modification of PARP1 as observed by the altered molecular weight of PARP1 on western blot (Fig. S3b; Gibbs-Seymour et al., 2016). To test whether such change in molecular weight of PARP1 is due to altered polymer length, we subjected the reaction mixture for ELTA labeling. Indeed, the addition of HPF1 reduced both the amount and length of PAR associated with PARP1 (Fig. 3b). Taken together, ELTA provides a sensitive approach to assess the polymer length of ADP-ribosylated proteins or complexes in their native modified state.

Next, we tested whether ELTA can be used to detect the length of PAR isolated from cells (Fig. 3c). PAR was isolated from cells using a solid-phase extraction method that allows for

the high recovery of PAR without any bias for different chain lengths (Martello et al., 2013). Human keratinocyte HaCaT cells were either untreated or H₂O₂-treated to induce PARylation, pre-treated with the PARP inhibitor Olaparib prior to H₂O₂, or pre-treated with PARG inhibitor PDD 00017273 (James et al., 2016) prior to H₂O₂. As a control, we also isolated PAR from *in vitro* modified *ha*PARP, which generates PAR of 2–25mer in length (Slade et al., 2011). As expected, we observed significant PAR signals in H₂O₂-treated cell samples (Fig. 3c; lane 3), which is longer than the one isolated from *ha*PARP (lane 1). PARP inhibitor Olaparib (lane 4) reduced the signal to background levels similar to the untreated cells (lane 2). On the contrary, PARG inhibition resulted in the enrichment of overall signals, confirming that the observed signals are indeed PAR (lane 5). Taking advantage of this novel approach to assess PAR length in cells, we labeled PAR isolated from 0, 2.5, 5, 7.5, and 10 min of H₂O₂-treatment and observed a distinctive shift in the profile of the polymer length over the time-course (Fig. S3c). Taken together, ELTA can be used to assess the length of PAR isolated from individual proteins or cells.

ELTA allows for selective labeling and enrichment of ADP-ribosylated peptides

Building on our findings that ELTA can be used to label protein-conjugated ADP-ribose (cf. Fig. 1d, e), we sought to develop a workflow for selective labeling and enrichment of ADP-ribosylated peptides from cell lysates, which may be applied to existing global ADP-ribosylated proteome analyses (Carter-O’Connell et al., 2014; Daniels et al., 2015a; Gibson et al., 2016; Larsen et al., 2018; Leidecker et al., 2016; Pedrioli et al., 2018; Martello et al., 2016; Westcott et al., 2017; Zhang et al., 2013; Zhen et al., 2017). We propose a pipeline composed of three steps that are illustrated in Fig. 4a: (1) the labeling of ADP-ribosylated peptides with the “clickable” dATP analog, N⁶-(N-azido)hexyl-dATP, by OAS1, (2) conjugation of OAS1-labeled peptides to dibenzocyclooctyne (DBCO)-agarose through copper-free click chemistry (Jewett and Bertozzi, 2010), and (3) treatment of agarose-conjugated peptides with *hs*NudT16 phosphodiesterase to release peptides, now possessing a phosphoribose tag at former sites of ADP-ribosylation, for mass spectrometry analysis (Daniels et al., 2015b).

First, we tested whether OAS1 can label a glutamine ADP-ribosylated peptide, HK533 (Kistemaker et al., 2016), with N⁶-(N-azido)hexyl-dATP and analyzed the reaction product by MALDI-TOF. As expected, a peak shift of 438.1 Da was observed (Fig. 4b, panel 1), which corresponds to N⁶-(N-azido)hexyl-dAMP. Next, we incubated this reaction with DBCO-agarose to allow for the conjugation of N⁶-(N-azido)hexyl-dAMP-labeled HK533 to the resin. We observed that there were no peaks in the mass range of N⁶-(N-azido)hexyl-dAMP-labeled HK533 in the flowthrough (Fig. 4b, red profile in panel 2), suggesting that a large proportion of the N⁶-(N-azido)hexyl-dAMP-labeled HK533 was conjugated to and pulled down by the DBCO-agarose. Consistently, the unlabeled HK533 peptide was present in the flowthrough of the sample not treated with OAS1 (Fig. 4b, black profile in panel 2), but absent in the sample treated with OAS1 (red profile). These data indicate that unlabeled HK533 is not significantly retained by the DBCO-agarose. To confirm the conjugation of N⁶-(N-azido)hexyl-dAMP-labeled HK533 peptide with the resin, we treated the peptide-conjugated DBCO-agarose resin with *hs*NudT16 (cf. Fig. 1d, e; Fig. 4a). We observed the largest peak (1529.9 m/z) at the expected m/z (1529.8) for phosphoribosylated HK533 in the

eluent of the peptide sample treated with OAS1 (Fig. 4b, red profile in panel 3) and no significant peaks in the sample without OAS1 (black profile). To test whether ELTA labeling is affected by the type of amino acid conjugated with ADP-ribose, we also tested a serine ADP-ribosylated peptide, JV-099 (Voorneveld et al., 2018; Fig. S4a, b). Similar efficiency in labeling and enrichment was observed, suggesting that the ELTA method can label peptide irrespective of the nature of the conjugated site or its neighboring residues.

Next, we assessed whether our workflow could be applied to enrich ADP-ribosylated peptides from lysates and identify the modification sites by liquid chromatography tandem mass spectrometry (LC-MS/MS). We added 1 nmol of HK533 into 1 mg of a tryptic digest of HeLa cell lysates (~1 μ mol total peptides) and used this complex peptide mixture as the input for ELTA-based enrichment workflow. LC-MS/MS analyses of the input and eluent demonstrated that the workflow resulted in the robust enrichment of molecular species with a retention time of ~6.5 min (Fig. 4c, panels 1 and 2). MS analysis of this peak demonstrated that it was predominantly composed of two species that matched the expected m/z for phosphoribosylated HK533 in the +2 and +3 charge states (Fig. 4c, panel 3). Subsequent MS/MS analyses confirmed the sequence and ADP-ribosylated site localization of HK533 (Fig. S4c). To test the sensitivity of our approach, we repeated the experiment by mixing 1 pmol or 1 fmol of HK533 into ~1 μ mol total peptides, where 50% of the samples were subjected for MS analyses. In each case, HK533 was identified (Fig. 4d), suggesting that our pipeline can identify ADP-ribosylated peptides with sub-femtomole sensitivity.

As an initial attempt to explore whether the current pipeline can also be used to enrich endogenous ADP-ribosylated peptides, we performed the ELTA-based enrichment workflow in triplicate using 2.5 mg of tryptic digest of H₂O₂-treated HeLa cell lysates as the input. As above, we labeled tryptic peptides with N⁶-(N-azido)hexyl-dATP by ELTA, conjugated the labeled peptide to DBCO-agarose, and eluted with *hsNudT16* that resulted in phosphoribosylated peptides for LC-MS/MS analyses. We identified 175 endogenous ADP-ribosylated peptides and 123 proteins in total (Table S1; Methods S1). Among the 123 proteins, 95 of them identified in previous studies based on cross-comparison with ADPriboDB (Vivelo et al., 2016). A statistically significant overlap was observed at a p-value of 7.3×10^{-98} using Fisher's exact test. Amongst them, 29 proteins were identified in two or more replicates, with ~90% overlap with ADPriboDB (26 proteins, $p = 6.3 \times 10^{-31}$; Table S1). This significant overlap corresponds to 35 out of 41 endogenous ADP-ribosylated peptides which are modified at a range of amino acids (e.g., Fig. 4e, see also Table S1 and Methods S1). Therefore, ELTA is capable of enriching for endogenous ADP-ribosylated peptides, which feature a variety of sequences on the peptide backbone and modified sites.

DISCUSSION

ELTA: an efficient, straightforward and versatile method to label free and protein-conjugated ADP-ribose

We report a novel enzymatic approach to label the 2'-OH terminus of ADP-ribose monomers and polymers. Though it has been possible to label ADP-ribose at its 1' aldehyde using a chemical approach (Fahrer et al., 2007), ELTA is an easy, efficient and straightforward method that could be used in conventional molecular biology labs without

special equipment or expertise. In addition, ELTA has now made it possible to label ADP-ribose that is also conjugated to a protein at the 1' position (cf. Fig. S1a). Since OAS1 accepts a range of commercially available dATP analogs as substrates, ELTA is a flexible tool that can incorporate standard molecular biology techniques that require the derivatization of the assayed molecule (e.g., radioactive, fluorescent, etc.) to study PAR. We have demonstrated several proof-of-concept applications: (1) the use of fluorescently labeled PAR of defined chain length for biophysical measurements; (2) radiolabeling of PAR isolated from cells or individual proteins to allow the detection of their associated polymer length; (3) the use of an azide tag to directly conjugate ADP-ribosylated peptides onto agarose beads by click chemistry for the downstream enrichment of ADP-ribosylated substrates and mass spectrometry identification. The possibility of covalently linking ADP-ribose or ADP-ribosylated protein to solid supports opens avenues for nanoparticle delivery or solid-phase chemistry. We noted that azido labeling also allows us to tap into the versatility of click chemistry for bioconjugation to any compatible substrates. Given that the synthetic routes for preparing various ATP derivatives are established (Bagshaw, 2001), it is foreseeable that similar dATP analogs can be made and applied to ELTA for new applications. For example, adding fluorine-19 for making an NMR probe or a diazine group for a photo-affinity probe (Bagshaw, 2001).

ELTA is distinct from other reagents, such as antibodies or protein domains, that recognize ADP-ribose (Affar et al., 1999; Gibson et al., 2017; Kawamitsu et al., 1984) in that it goes beyond functioning as a detection reagent. ELTA allows researchers to modify ADP-ribose with a variety of labels that allows for further measurement, enrichment as well as detection. While antibodies are developed against PAR of specific ADP-ribose length (Affar et al., 1999; Kawamitsu et al., 1984) and protein domains may have sequence specificities beyond the protein-conjugated ADP-ribose (Forst et al., 2013; Moyle and Muir, 2010), ELTA targets a chemical group that is present in various forms of ADP-ribose (i.e., 2'-OH terminus), which allows quantitative comparisons between different forms based on detection of a consistent tag (e.g., biotin).

ELTA simplifies the measurement, detection and enrichment of ADP-ribosylation

Currently, ELTA can be used to effectively label sub-femtomole levels of ADP-ribose, thereby allowing for efficient labeling of limited materials for downstream analyses. We have demonstrated the use of radioactive and fluorescent PAR of defined length for measurement of the equilibrium dissociation constant with a PAR-binding module using filter binding assays and MST, respectively. We note that only trace amounts of labeled PAR polymers are required compared to the current methods that require large quantities of PAR polymers that are often outside the reach of most academic laboratories. These labeled molecules can also be used for single molecule-based measurement (Chen and Larson, 2016) or intracellular tracking of PAR (Krukenberg et al., 2015). When combined with the existing chemical approach to label PAR at 1' position, ELTA can be used to attach functionalities at both termini. Such a dual labeling approach has been transformative for studying DNA and RNA biology, and, therefore, ELTA may now open the possibility for PAR to serve as a building block in synthetic biology, such as creating model ADP-ribosylated proteins with a defined PAR length. Given that ELTA labels the 2'-OH terminus

and that some PARPs create branched points resulting in additional 2'-OH groups from a single 1'' terminus, labeling at both 1'' and 2' ends may help in determining the branching frequency of intact PAR polymers isolated from individual proteins or cells.

Several methods have been developed to measure the length of PAR chain from cells; however, the majority of them require the digestion of PAR into monomeric nucleosides prior to analyses (Juarez-Salinas et al., 1979; Kanai et al., 1982; Keith et al., 1990; Martello et al., 2013; Shah et al., 1995), thereby losing the information of length distribution of intact PAR chains. Alternatively, it is possible to measure the length of intact PAR chains from cells by feeding them with radiolabeled adenine (Aboul-Ela et al., 1988; Alvarez-Gonzalez and Jacobson, 1987). However, this approach suffers from several drawbacks, including non-specific labeling of other polynucleotides (DNA and RNA) and potential induction of PAR signals by the radiodamage of DNA (Martello et al., 2013). Nucleic acid staining such as silver stain and SYBR Gold are, on the other hand, insensitive to very short chains (*cf.* Fig. S1d and S3a); as their signals are approximately correlated to the number of the ADP-ribose groups present in the PAR chain, these methods may not be useful for quantifying the differences between PAR of different chain lengths. Using ELTA, a single radioactive label is added to the end of a 2'-OH terminus and, therefore, the signal observed is directly correlated to the number of 2'-OH termini of PAR of any given individual length. Though multiple 2'-OH termini may be present due to PAR branching, the quantitation of different chain lengths will likely be minimally affected as branching occurs at a level of 1–2% (Martello et al., 2013). As PARP inhibitors are currently used to treat cancer patients and in clinical trials for other diseases, ELTA can help evaluate the effect of these drugs on cellular ADP-ribosylation comprehensively—i.e., by monitoring changes of both site and length of ADP-ribosylation. We found that PAR length distribution reduced significantly by PARP inhibitors and PAR accumulated with an altered profile upon PARG inhibition. Whether the latter profile change is related to the differential processivity of PARG activity observed for different PAR length in vitro (Brochu et al., 1994) warrants further investigation. Notably, FDA-approved PARP inhibitors, including Niraparib and Olaparib, have clinical efficacy and accumulate DNA damage only when the PAR level is reduced by >90% (Moulder and Hedley, 2016). One possible interpretation is that a longer PAR chain can still result in DNA repair, but not a shorter one, consistent with previous observations that DNA repair factors bind to PAR in a length-selective manner (Fahrer et al., 2007; Leung, 2014; Min et al., 2013; Popp et al., 2013). Therefore, it will be interesting to explore whether PAR length distribution could be an important biomarker for the clinical effectiveness of these inhibitors.

Beyond free and protein-conjugated ADP-ribose

In summary, we demonstrated that ELTA can be used to label free and protein-conjugated ADP-ribose and provided examples of its applications. However, this novel technique may have broader applications for ADP-ribose metabolism. Besides protein-conjugated ADP-ribose, studies in prokaryotes and eukaryotes have revealed several ADP-ribose derivatives that have free 2'-OH groups, including O-acetyl-ADP-ribose generated by the sirtuin deacetylase family, ADP-ribose-1''-phosphate from tRNA splicing, ADP-ribosylation of the antibiotics rifamycin, as well as the recently discovered DNA ADP-ribosylation (reviewed in Palazzo et al., 2017). ELTA may, therefore, provide a timely tool for discovering the

functions of these various forms of ADP-ribosylation in antibiotic resistance, as well as NAD⁺, RNA, and DNA metabolism.

LIMITATIONS

We have developed a robust method to label protein-conjugated and free ADP-ribose enzymatically. As in any labeling methods, the label itself, however, may affect the binding of protein partners. Therefore, any measurement with the labeled molecules should be verified independently with existing methods (*cf.* Fig. 2). Even though ELTA can be used to label sub-femtomole of ADP-ribose, the detection is limited by the choice of the label attached (e.g., fluorescent or radioactive) and the sensitivity of the detector available. If weak signals need to be amplified for detection, ATP can potentially be used in place of dATP to form oligomers on ADP-ribose (Cayley and Kerr, 1982). However, this approach will be at the expense of the linear response of ELTA, which exhibits a 1:1 relationship between observed signals and 2'-OH terminus present in ADP-ribose.

STAR★Methods

Contact for Reagent and Resource Sharing

Further information and requests for resources and reagents should be directed to and will be fulfilled by the Lead Contact Anthony K. L. Leung (anthony.leung@jhu.edu).

Protein expression and purification

Human OAS1—Full length human 2'-5'-oligoadenylate synthase 1 (OAS1, UniProtKB P00973) codon optimized for insect cell expression into the MultiBac pFl vector (Bieniossek et al., 2008) with Strep-Sumo tag followed by TEV cleavage site. SF9 cells were infected with baculovirus expressing OAS1 for 72 h. The protein was purified using StrepTactin resin (IBA bioTAGnology) followed by Strep-Sumo tag removal using TEV protease. The protein was further purified by gel filtration using a HiLoad 16/60 superdex 200 column. The protein was flash frozen in a buffer containing 50 mM Tris pH 8.0, 100 mM NaCl, 5 mM DTT and 10% glycerol, and stored at -80°C until use.

Automodified PARPs—Recombinant PARP1, PARP10^{CD}, *hsNudT16*, *haPARP* proteins were purified as described previously (Daniels et al., 2015b; McPherson et al., 2017; Slade et al., 2011). The automodification of PARPs was performed as described (Daniels et al., 2014; McPherson et al., 2017). Briefly, PARylated PARP1 proteins were prepared in a reaction buffer containing 20 mM Tris-HCl pH 7.5, 50 mM NaCl, 5 mM MgCl₂, 10 mM β-mercaptoethanol, 1 mM NAD⁺ and 2 μM 1x activated DNA (Trevigen) with or without 3 μCi ³²P-NAD⁺. The mixtures were incubated at 30°C for 30 min and 20 μM Olaparib added to stop the reaction. MARYlated PARP10^{CD} proteins were prepared in a reaction buffer containing 20 mM Tris-HCl pH 7.5, 50 mM NaCl, 5 mM MgCl₂, 10 mM β-mercaptoethanol and 1 mM NAD⁺. The mixtures were incubated at 37°C for 2 h. Excess NAD⁺ was removed by desalting in a Zeba Spin Desalting Columns (Thermo Fisher Scientific) equilibrated with the reaction buffer. PARylated *haPARP* proteins were prepared in a reaction containing 18 μM *haPARP*, 50 mM Tris-HCl pH 7.5, 50 mM NaCl, 1x activated DNA and 3.5 mM NAD⁺.

The mixture was incubated at 25°C, 500 rpm for 1 h. Excess NAD⁺ was removed by desalting into 50 mM Tris pH 7.5, 50 mM NaCl with a HiTrap desalting column (GE healthcare) on an NGC 100 medium-pressure chromatography system (Bio-Rad).

RNF146 WWE domain—The WWE domain of human RNF146 was cloned into pET28a vector with His-Sumo tag followed by TEV protease cleavage site. The protein was expressed at 18°C for 16 h. The protein was initially purified using NiNTA resin (Qiagen) followed by His-Sumo removal with TEV protease. The protein was further purified on SP HP cation exchange column (GE healthcare) followed by HiLoad 16/60 superdex 75 size exclusion column (GE healthcare). The protein was flash frozen in a buffer containing 50 mM Tris pH 8.0, 100 mM NaCl, 5 mM DTT and 10% glycerol and stored at –80°C until use.

HPLC fractionation of PAR

PAR was synthesized as previously described (Tan et al., 2012). For the fractionation of PAR, a semi-preparative DNAPac PA100 column (9 × 250 mm) was used to fractionate PAR into homogeneous polymers. Approximately 2.74 μmol (~3 mg) of PAR was loaded onto the column equilibrated with Dionex buffer A (25 mM Tris-HCl pH 9.0), and the concentration of Dionex buffer B (25 mM Tris-HCl pH 9.0 and 1M NaCl) in a 120-min method was set to elute as follows: 0 min (0% B), 6 min (0% B), 10 min (30% B), 60 min (40% B), 78 min (50% B), 108 min (56% B), 112 min (100% B), 114 min (100% B), 115 min (0% B), 120 min (0% B). The 2-ml fractions were collected and concentrated using Amicon Ultra centrifugal filters (Sigma Aldrich).

Labeling of free ADP-ribose with dATP analogs using OAS1

For radiolabeling, ADP-ribose, NAD⁺, *iso*-ADP-ribose (10 μM each), or PAR (25 μM each) were reacted with 5 μCi α-³²P-dATP (Perkin-Elmer), 50 μg/mL low molecular weight (LMW) poly(I:C) (Invivogen). Addition of poly(I:C) (synthetic dsRNA analog) is critical as it activates OAS1 (Lohöfener et al., 2015). The labeling reaction started by adding 50 μg/mL OAS1 in 1x labeling buffer (20 mM Tris-HCl pH 7.5, 20 mM Magnesium Acetate, 2.5 mM DTT) at 37°C for 2 h. The samples were resolved on 7 M urea 15% polyacrylamide gel followed by autoradiography. For labeling with Cy3-dATP, 10 μM ADP-ribose or PAR were incubated with 4 μM Cy3-dATP (Perkin Elmer), 50 μg/mL LMW poly(I:C) and 50 μg/mL OAS1 in 1x labeling buffer at 37°C for 2 h. The samples were separated on 7 M urea 15% polyacrylamide gel and visualized using a Typhoon FLA7000 machine (GE HealthCare). For biotin labeling, 10 μM PAR was incubated with 40 μM biotin-14-dATP (ThermoFisher Scientific), 50 μg/mL LMW poly(I:C), 50 μg/mL OAS1 in 1x labeling buffer. The samples were applied to Illustra MicroSpin G-25 columns (GE HealthCare) to remove free biotin-14-dATP and detected by IR dye 800CW Streptavidin (Li-Cor Biosciences) and anti-PAR polyclonal antibodies (Trevigen) using dot blot.

Single-length PAR radiolabeling with α-³²P-dATP was performed in a reaction consisting of 20 mM Tris pH 7.5, 20 mM Magnesium Acetate, 2.5 mM DTT, 0.6 M purified OAS1, 0.5 mg/ml LMW poly (I:C), 0.05 M PAR, and 0.33 M of dATP, [α-³²P]- 3000Ci/mmol. The reaction was incubated for 2 h at 37°C, and then the excess of radiolabeled dATP was

removed using Illustra MicroSpin G-25 columns. Single-length PAR labeling with Cy5 was performed under the same conditions but with 1 M PAR and 10 M of either N6-(6-Amino)hexyl-dATP -Cy5 (Jena BioSciences) or 10 M of Cy5-dATP (PerkinElmer). For Cy5-dATP calibration curve, 1:2 serial dilutions of Cy5-dATP (Perkin-Elmer) were measured and fluorescence was plotted using Prism 6 (GraphPad). Cy5-PAR fluorescence was then measured, and PAR concentration was calculated using the linear curve equation of the Cy5-dATP calibration curve ($F_{norm} = 2077 * [nM] - 131.6$). To remove poly(I:C) for purified PAR, KCl was added to the labeled PAR to a final concentration of 100 mM and poly(I:C) was removed by RNase R digestion at 37°C for 1 h. Labeled PAR was then extracted using Trizol-LS reagent (ThermoFisher Scientific) or RiboZol RNA extraction kit (VWR).

Labeling of ADP-ribosylated proteins with dATP analogs using OAS1

1 µg automodified proteins (without ^{32}P -NAD⁺) or the negative control BSA was labeled with 4 µCi ^{32}P -dATP, 4 µM Cy3-dATP or 40 µM biotin-14-dATP by 50 µg/mL OAS1 at 37°C for 2 h. For demodification, automodified proteins were treated with *hsNudT16* proteins at 37°C for 1 h and then labeled with dATP analogs. The protein samples were separated on SDS-PAGE. Total protein levels were analyzed with SimplyBlue Safe Stain (Thermo Fisher Scientific).

Isolation of ^{32}P -labeled PAR from PARP1 proteins

1 µg automodified PARP1 proteins (without ^{32}P -NAD⁺) was precipitated with TCA and labeled with 4 µCi ^{32}P -dATP by incubation with 50 µg/mL OAS1 at 37°C for 2 h. PAR chains were isolated from the ^{32}P -NAD⁺ labeled PARP1 or ^{32}P -dAMP labeled PARP1 proteins by shaking with PAR release buffer (1 M KOH and 50 mM EDTA) at 60°C for 2 h. PAR solutions were neutralized with HCl to pH 7.5 followed by phenol-chloroform purification and ethanol precipitation. The pellets were dissolved in water, and the samples were purified with Illustra MicroSpin G-25 columns.

ELTA Labeling of PAR isolated from individual proteins and cells

For PAR isolated from *in vitro* modified *ha*PARP, 100 µg of *ha*PARP was incubated with 5 mM NAD⁺ and 1x activated DNA for 2 h at 30°C in automodification buffer (50 mM Tris-HCl pH 7.5, 50 mM NaCl). Modified protein was precipitated by 20% (w/v) cold TCA and stayed on ice for 15 min. Pellet was centrifuged at 14000xg for 15 min, washed with 70% ethanol, and air-dried. For PAR isolated from cells, 1.0×10^6 HaCaT cells were seeded in 10 cm dishes. When 90% of cell confluence was reached, cells were either treated with or without 1 mM H₂O₂ for 10 min. In addition, 20 µM PARP inhibitor Olaparib or 1 µM PARG inhibitor PDD 00017273 were added in DMEM containing 10% FBS for 2 h, then treated with 1 mM H₂O₂ for 10 min. For the time-course experiment, 1.0×10^6 HaCaT cells were seeded in 10 cm dish. When 90% of cell confluence was reached, cells were treated with 1 mM H₂O₂ for 0, 2.5, 5, 7.5, and 10 minutes. In all cases, cells were washed by ice-cold 1x PBS, and cellular proteins were precipitated by 20% (w/v) cold TCA and stayed on ice for 15 min. Pellets were centrifuged at 3000xg for 10 min, washed by 70% ethanol, and air-dried. PAR isolated from *in vitro* modified proteins or from cells was then extracted by 0.5 M KOH digestion at 37°C for 90 min and neutralized by 0.8 M MOPS buffer. To digest

nucleic acids and proteins, samples were treated with 0.08 mg/mL DNase and 0.08 mg/mL RNase A for 3 h at 37°C, followed by incubated with 0.16 mg/mL Proteinase K overnight. Samples were then purified by High Pure miRNA Isolation Kit (Roche) to enrich samples for PAR as previously described (Martello et al., 2013). 100 µL of Milli-Q water was used for sample elution.

For characterizing PAR isolated from PARP1 automodification with and without HPF1, recombinant PARP1 and HPF1 proteins were purified as previously described (Langelier et al 2011, Gibbs-Seymour et al 2015). In a 0.25 mL reaction, PARP1 (10 µM) with HPF1 (10 µM) or BSA (10 µM) were prepared in a reaction buffer containing 20 mM Tris-HCl pH 7.5, 50 mM NaCl, 5 mM MgCl₂, 10 mM β-mercaptoethanol, 1 mM NAD⁺ 2 and 10 µM duplex DNA. The mixtures were incubated at 25°C for 20 min and an equal volume of ice-cold 20% TCA was used to stop the reaction. The samples were put on ice for 15 minutes. Proteins were precipitated by spinning at 9,000 xg, 4 °C for 10 minutes. Precipitated proteins were washed once with ice-cold 70°C ethanol then air-dried. Pellets were resuspended in 255 µL 0.5 M KOH and incubated at 37°C for 10 minutes. After neutralization with 50 µL 4.8 M MOPS buffer, MgCl₂ (5 mM) and DNase I (0.1 mg/mL) were added and the samples were incubated at 37 °C for 2 hours. CaCl₂ (1 mM) and proteinase K (0.2 mg/mL) were added and the samples were incubated at 37 °C overnight. PAR isolation was performed with the High Pure miRNA isolation kit (Roche) and was eluted with 50 µL Milli-Q water. PAR isolated from PARP-1 (5 µL, diluted 1:15 in mQ water) or from PARP-1 + HPF1 (5 µL) was labeled with [α -³²P]-dATP (4 µCi) and dATP (50 µM) as above. Samples were incubated in denaturing PAGE buffer at 70 °C for 10 minutes, then separated on a 15% denaturing polyacrylamide gel.

Silver Staining

PAR samples were resolved on 7M urea 15% polyacrylamide gels. After electrophoresis, the gel was fixed overnight in 50% ethanol and 5% acetic acid, following by a 30 min wash by Milli-Q water for 4 times the next day. The stain was performed by using Pierce™ Color Silver Stain Kit (ThermoFisher Scientific). In brief, silver reagent was applied for 30 min, following by a short rinse of water for 10 s. An equal amount of reducer base reagent and reducer aldehyde reagent was then mixed and applied to the gel for 3–5 min. The gel was washed with Milli-Q water to reduce the background, and stabilizer reagent was added for another 30 min.

Filter binding Assays

Defined length ³²P-labeled PAR chain (200 pM) was incubated with 2-fold serial dilutions (20 µM to 0.6 nM) of RNF146 WWE domain. Samples were applied to a slot blot apparatus as described (Elkayam et al., 2017). The protein–PAR complex was captured on a nitrocellulose membrane, and the free PAR was captured on a subsequent nylon membrane. The protein-bound and unbound radiolabeled PAR were visualized by phosphorimaging (Typhoon 7000, GE Healthcare) and quantified using GeneTools software (Synoptics). The results of three experiments were analyzed using Prism 6 software (GraphPad). Data are shown as means of bound PAR/(bound PAR+unbound PAR) ± standard deviation (SD).

MST analyses

Defined length Cy5-labeled PAR chain (500 pM) was incubated with 2-fold serial dilutions (20 μ M to 0.6 nM) of RNF146 WWE domain. Binding was measured using Monolith NT. 115 pico (NanoTemper) at 20% excitation power and 40% MST power. Data are shown as means of Normalized fluorescence \pm SD.

MALDI-TOF analyses

For MALDI-TOF analysis of OAS1-labeled ADP-ribose, 1 mM ADP-ribose was incubated with 1 mM dATP (Sigma-Aldrich), 20 μ g/mL LMW poly(I:C), and 20 μ g/mL OAS1 in 1 \times labeling buffer at 37°C for 1 h. After incubation, reactions with ADP-ribose were diluted 1:4 in a solution containing 80% acetonitrile (ACN; Sigma-Aldrich), 0.1% trifluoroacetic acid (TFA; Sigma-Aldrich) and 10 mg/mL 2,5-dihydroxybenzoic acid (DHB; Sigma-Aldrich). Samples containing ADP-ribose were analyzed by MALDI-TOF (Applied Biosciences Voyager) in reflector, positive-ion mode accelerated at 20 kV with a 65.5% grid and 500 Da mass cutoff. HK533 [ac-PQ(ADPr)PAKSAPAPKKG-am] and JV-099 [ac-PAKS(ADPr)APAPKKG-am] were synthesized as previously described (Kistemaker et al., 2016; Voorneveld et al., 2018) and resuspended in Milli-Q H₂O. For analysis of OAS1-labeled ADP-ribosylated peptides, ~100 pmol of HK533 or JV-099 in 1 μ L was diluted 1:4 in a solution containing 80% ACN, 0.1% TFA and 10 mg/mL DHB. For analysis of samples concentrated on StageTips (Fig. 4b, flowthrough and elution), samples were eluted from StageTips with 5 μ L of 80% ACN, 0.1% TFA and diluted 1:1 in a solution containing 80% ACN, 0.1% TFA and 10 mg/mL DHB. All peptide samples were spotted on a MALDI-TOF plate and allowed to dry at room temperature. Samples were analyzed by MALDI-TOF in the reflector, positive-ion mode accelerated at 20 kV with a 65.5% grid and 1000 Da mass cutoff.

Cell harvesting, proteolysis, and desalting for proteomic analyses

Endogenous ADP-ribosylation was induced in HeLa cells by treatment with 1 mM H₂O₂ in DMEM supplemented with 10% FBS at 37°C for 10 min. HeLa cells were washed once in ice-cold 1x PBS and harvested and lysed in 50 mM Tris pH 7.4, 400 mM NaCl, 1 mM EDTA, 1% NP-40, 0.1% sodium deoxycholate with 1x SigmaFast protease inhibitor (Sigma-Aldrich). Insoluble material was cleared by centrifugation and proteins in the soluble fraction were precipitated by diluting in a five-fold volume of 100% acetone and stored at -20°C overnight. The precipitant was solubilized in 10 mM HEPES pH 8.0, 8 M urea. Protein concentration was determined by Bradford assay and adjusted to 5 mg/mL. Proteins were then reduced and alkylated with 1 mM TCEP and 6 mM 2-chloroacetamide for 1 h at room temperature. The sample was then diluted eight-fold in 25 mM ammonium bicarbonate; trypsin (Pierce) and LysC (Wako) were added at a 1:100 enzyme:substrate ratio (w/w) and incubated at 37°C overnight. Samples were then acidified to pH 2 with 10% TFA and loaded onto a SepPak C18 Classic cartridge conditioned with methanol and equilibrated with 0.1% TFA. Immobilized samples were washed with 10 mL 0.1% TFA followed by 30 mL of Milli-Q H₂O and eluted with 3 mL of 80% ACN. Samples were dried by vacuum centrifugation to approximately 200 μ L and quantified by A₂₈₀ prior to further use.

OAS1 labeling, enrichment, and elution of ADP-ribosylated peptide HK533

Specified amounts of HK533 (5 nmol for MALDI-TOF, 1 nmol or less for LC-MS/MS) were incubated with 100 μM N^6 -(6-Azido)hexyl-dATP (Jena Bioscience), 20 $\mu\text{g}/\text{mL}$ LMW poly(I:C), and 20 $\mu\text{g}/\text{mL}$ OAS1 in 1x labeling buffer at 37°C for 1 h. For experiments where HK533 was enriched from cell lysate peptides, 1 mg of peptides generated from untreated HeLa cells were added to the reaction at a final concentration of 10 mg/mL. For experiments enriching for endogenous ADP-ribosylated peptides, 2.5 mg of peptides generated from H_2O_2 -treated HeLa cells were added to the reaction at a final concentration of 8.33 mg/mL. All OAS1 reactions were then added to 30 μL DBCO-agarose (Click Chemistry Tools) equilibrated and resuspended in 300 μL 1x PBS and rotated end-over-end at room temperature for 1 h. The samples were briefly centrifuged to pellet the resin, and the supernatant (flowthrough) was removed and concentrated on StageTips conditioned with 80% ACN, 0.1% TFA and equilibrated in 0.1% TFA. StageTips were washed once with 5% ACN, 0.1% TFA and stored at 4°C prior to further analysis. By this method, the resin was washed thrice with 5M NaCl, and then thrice with 20% ACN containing 0.1% TFA, and finally thrice with 1x PBS. The resin was resuspended in 200 μL of 100 mM HEPES pH 8.0, 15 mM MgCl_2 . 8 μg of recombinant *hsNudT16* was added, and the samples were incubated at 37°C for 2 h shaking at 1400 rpm. The samples were briefly centrifuged to pellet the resin, and the supernatant was concentrated and desalted on StageTips as described above.

LC-MS/MS analysis

For LC-MS/MS analysis, peptides were eluted from StageTips with 50 μL of 80% ACN and 0.1% TFA, dried by vacuum centrifugation and resuspended in 10 μL of 5% ACN and 0.1% TFA. Peptides were separated on a 75 $\mu\text{m} \times 150$ mm ProntoSIL-120-5-C18 H column (5 μm , 120 Å, BISHOFF) using a 2–30% ACN gradient in 0.1% acetic acid at 300 nl/min over 90 min and analyzed on a Thermo Scientific Q Exactive Plus mass spectrometer for analysis of HK533 or a Thermo Scientific Fusion Orbitrap for analysis of endogenous ADP-ribosylated peptides interfaced with an Easy-nLC 1000 (Thermo Fisher Scientific). For analysis of HK533 data-dependent analysis was applied using Top15 selection and fragmentation was induced by HCD with collision energy set to 28%. Peptides were identified from isotopically resolved masses in MS and MS/MS spectra at resolutions of 70,000 and 35,000, respectively. For analysis of endogenous ADP-ribosylated peptides data-dependent analysis was applied using Top15 selection and fragmentation of precursors with a +2 charge state was induced by HCD with collision energy set to 30% and fragmentation of precursors with a +3 charge state or higher was induced by EThCD. Peptides were identified from isotopically resolved masses in MS and MS/MS spectra at resolutions of 120,000 and 30,000, respectively.

Database search of MS/MS spectra for identification of ADP-ribosylated peptide

Raw files were analyzed by MaxQuant version 1.5.7.4 using protein, peptide, and site FDRs of 0.01 and a score minimum of 40 for modified peptides and 0 for unmodified peptides and delta score minimum of 17 for modified peptides and 0 for unmodified peptides. Sequences from HK533 experiments were searched against a FASTA file containing the sequence of synthetic ADP-ribosylated peptide HK533. MaxQuant search parameters were set to match

the chemical modifications of HK533 and included: variable modifications at acetylation (N-term), amidation (C-term) and phosphoribosylation (Q). Sequences from endogenous peptide experiments were searched against a UniProt FASTA file of the human proteome. MaxQuant search parameters were set with variable modifications at acetylation (Protein N-term), oxidation (M) and phosphoribosylation (DEKRSY) and a fixed modification of carbamidomethylation (C). Phosphoribosylation was defined as a modification of C₅H₉PO₇ (212.009). Max-labeled amino acids were 3, max missed cleavages were 2, enzyme was Trypsin/P, max charge was 7, multiplicity was 2.

Supplementary Material

Refer to Web version on PubMed Central for supplementary material.

ACKNOWLEDGEMENTS

We thank Paul Chang, Joel Moss, Marc Greenberg and the members of the Leung lab for their critiques of the manuscript, Vinay Ayyappan for maintaining ADPriboDB used in this analysis, and Mohsen Badiie for drawing the schematics of Figure 1a. We thank Timothy Mitchison, Edwin Tan and Kristin Krukenberg for sharing *in vitro* purified PAR and their advice for synthesizing and purifying PAR to defined chain length. We thank Ivan Ahel for the plasmid encoding *ha*PARP, Wenqing Xu for *iso*-ADP-ribose and Hans Kistemaker for the ADP-ribosylated peptide HK533. We thank Bob Cole in the Mass Spectrometry and Proteomics Facility at the Johns Hopkins School of Medicine for assisting mass spectrometry analyses and Arthur Makarenko from the CSHL mass spectrometry core facility for his help with PAR purifications using HPLC. We thank Anna Kondratova for pointing out a previous observation by Cayley and Kerr on the addition of oligoadenylate on ADP-ribose by OAS1 (Cayley and Kerr, 1982). This work was supported by a Johns Hopkins Discovery Award (A.K.L.L.), the Proteomics Core Coins Award from the Johns Hopkins School of Medicine (A.K.L.L. and R.L.M), W. W. Smith Charitable Trust Medical Research Award (A.K.L.L.), and research grants Research Scholar Award [RSG-16-062-01-RMC] (A.K.L.L.) from American Cancer Society, R01GM104135 (A.K.L.L), T32CA009110 (R.L.M), T32GM080189 (M.D.), and R01AR065459 (S.-E.O.) from the National Institutes of Health. Part of this work utilized an EASY-nLC1200 UHPLC and Thermo Scientific Orbitrap Fusion Lumos Tribrid mass spectrometer purchased with funding from a National Institutes of Health SIG grant S10OD021502 (S.-E.O.). L.J. is an Investigator of the Howard Hughes Medical Institute.

REFERENCES

- Aboul-Ela N, Jacobson EL, Jacobson MK, 1988 Labeling methods for the study of poly- and mono(ADP-ribose) metabolism in cultured cells. *Anal Biochem* 174, 239–250. [PubMed: 3218735]
- Affar EB, Duriez PJ, Shah RG, Winstall E, Germain M, Boucher C, Bourassa S, Kirkland JB, Poirier GG, 1999 Immunological determination and size characterization of poly(ADP-ribose) synthesized *in vitro* and *in vivo*. *Biochim Biophys Acta* 1428, 137–146. [PubMed: 10434031]
- Alvarez-Gonzalez R, Jacobson MK, 1987 Characterization of polymers of adenosine diphosphate ribose generated *in vitro* and *in vivo*. *Biochemistry* 26, 3218–3224. [PubMed: 3038179]
- Bagshaw C, 2001 ATP analogues at a glance. *J Cell Sci* 114, 459–460. [PubMed: 11171313]
- Ball LA, White CN, 1979 Induction, Purification, and Properties of 2'5'-Oligoadenylate Synthetase, in: Koch G, Richter D (Eds.), *Regulation of Macromolecular Synthesis by Low Molecular Weight Mediators*. Academic Press, pp. 303–317.
- Barkauskaite E, Jankevicius G, Ladurner AG, Ahel I, Timinszky G, 2013 The recognition and removal of cellular poly(ADP-ribose) signals. *FEBS J* 280, 3491–3507. doi:10.1111/febs.12358 [PubMed: 23711178]
- Berger NA, Besson VC, Boulares AH, Bürkle A, Chiarugi A, Clark RS, Curtin NJ, Cuzzocrea S, Dawson TM, Dawson VL, Haskó G, Liaudet L, Moroni F, Pacher P, Radermacher P, Salzman AL, Snyder SH, Soriano FG, Strosznajder RP, Sümegei B, Swanson RA, Szabó C, 2017 Opportunities for the repurposing of PARP inhibitors for the therapy of non-oncological diseases. *Br. J. Pharmacol* doi:10.1111/bph.13748

- Bieniossek C, Richmond TJ, Berger I, 2008 MultiBac: multigene baculovirus-based eukaryotic protein complex production. *Curr Protoc Protein Sci Chapter 5, Unit 5.20–5.20.26* doi: 10.1002/0471140864.ps0520s51
- Bilan V, Leutert M, Nanni P, Panse C, Hottiger MO, 2016 Combining HCD and EThcD fragmentation in a product dependent-manner confidently assigns proteome-wide ADP-ribose acceptor sites. *Anal Chem* doi:10.1021/acs.analchem.6b03365
- Bock FJ, Todorova TT, Chang P, 2015 RNA Regulation by Poly(ADP-Ribose) Polymerases. *Molecular Cell* 58, 959–969. doi:10.1016/j.molcel.2015.01.037 [PubMed: 26091344]
- Brochu G, Duchaine C, Thibeault L, Lagueux J, Shah GM, Poirier GG, 1994 Mode of action of poly(ADP-ribose) glycohydrolase. *Biochim Biophys Acta* 1219, 342–350. [PubMed: 7918631]
- Carter-O’Connell IO, Jin H, Morgan RK, David LL, Cohen MS, 2014 Engineering the substrate specificity of ADP-ribosyltransferases for identifying direct protein targets. *J Am Chem Soc.* doi: 10.1021/ja412897a
- Cayley PJ, Kerr IM, 1982 Synthesis, characterisation and biological significance of (2’–5’)oligoadenylate derivatives of NAD⁺, ADP-ribose and adenosine(5’’)tetraphospho(5’’)adenosine. *Eur J Biochem* 122, 601–608. [PubMed: 6277637]
- Chen H, Larson DR, 2016 What have single-molecule studies taught us about gene expression? *Genes Dev* 30, 1796–1810. doi:10.1101/gad.281725.116 [PubMed: 27601529]
- Cohen MS, Chang P, 2018 Insights into the biogenesis, function, and regulation of ADP-ribosylation. *Nat Chem Biol* 14, 236–243. doi:10.1038/nchembio.2568 [PubMed: 29443986]
- Daniels CM, Ong S-E, Leung AKL, 2015a The Promise of Proteomics for the Study of ADP-Ribosylation. *Molecular Cell* 58, 911–924. doi:10.1016/j.molcel.2015.06.012 [PubMed: 26091340]
- Daniels CM, Ong S-E, Leung AKL, 2014 Phosphoproteomic approach to characterize protein mono and poly(ADP-ribosyl)ation sites from cells. *J Proteome Res* 13, 3510–3522. doi:10.1021/pr401032q [PubMed: 24920161]
- Daniels CM, Thirawatananond P, Ong S-E, Gabelli SB, Leung AKL, 2015b Nudix hydrolases degrade protein-conjugated ADP-ribose. *Sci Rep* 5, 18271. doi:10.1038/srep18271 [PubMed: 26669448]
- Donovan J, Dufner M, Korennykh A, 2013 Structural basis for cytosolic double-stranded RNA surveillance by human oligoadenylate synthetase 1. *Proc Natl Acad Sci USA* 110, 1652–1657. doi: 10.1073/pnas.1218528110 [PubMed: 23319625]
- Elkayam E, Parmar R, Brown CR, Willoughby JL, Theile CS, Manoharan M, Joshua-Tor L, 2017 siRNA carrying an (E)-vinylphosphonate moiety at the 5’ end of the guide strand augments gene silencing by enhanced binding to human Argonaute-2. *Nucleic Acids Res* 45, 3528–3536. doi: 10.1093/nar/gkw1171 [PubMed: 27903888]
- Fahrer J, Kranaster R, Altmeyer M, Marx A, Bürkle A, 2007 Quantitative analysis of the binding affinity of poly(ADP-ribose) to specific binding proteins as a function of chain length. *Nucleic Acids Res* 35, e143. doi:10.1093/nar/gkm944 [PubMed: 17991682]
- Fahrer J, Popp O, Malanga M, Beneke S, Markovitz DM, Ferrando-May E, Bürkle A, Kappes F, 2010 High-affinity interaction of poly(ADP-ribose) and the human DEK oncoprotein depends upon chain length. *Biochemistry* 49, 7119–7130. doi:10.1021/bi1004365 [PubMed: 20669926]
- Feijs KLH, Forst AH, Verheugd P, Lüscher B, 2013 Macrodomein-containing proteins: regulating new intracellular functions of mono(ADP-ribosyl)ation. *Nat Rev Mol Cell Biol* 14, 445–453. doi:doi: 10.1038/nrm3601
- Ferbus D, Justesen J, Besançon F, Thang MN, 1981 The 2’5’ oligoadenylate synthetase has a multifunctional 2’5’’ nucleotidyl-transferase activity. *Biochem Biophys Res Commun* 100, 847–856. [PubMed: 6268077]
- Forst AH, Karlberg T, Herzog N, Thorsell A-G, Gross A, Feijs KLH, Verheugd P, Kursula P, Nijmeijer B, Kremmer E, Kleine H, Ladurner AG, Schüler H, Lüscher B, 2013 Recognition of mono-ADP-ribosylated ARTD10 substrates by ARTD8 macrodomains. *Structure* 21, 462–475. doi:10.1016/j.str.2012.12.019 [PubMed: 23473667]
- Gibbs-Seymour I, Fontana P, Rack JGM, Ahel I, 2016 HPF1/C4orf27 Is a PARP-1-Interacting Protein that Regulates PARP-1 ADP-Ribosylation Activity. *Molecular Cell* 62, 432–442. doi:10.1016/j.molcel.2016.03.008 [PubMed: 27067600]

- Gibson BA, Conrad LB, Huang D, Kraus WL, 2017 Generation and Characterization of Recombinant Antibody-like ADP-Ribose Binding Proteins. *Biochemistry*. doi:10.1021/acs.biochem.7b00670
- Gibson BA, Zhang Y, Jiang H, Hussey KM, Shrimp JH, Lin H, Schwede F, Yu Y, Kraus WL, 2016 Chemical genetic discovery of PARP targets reveals a role for PARP-1 in transcription elongation. *Science*. doi:10.1126/science.aaf7865
- Gupte R, Liu Z, Kraus WL, 2017 PARPs and ADP-ribosylation: recent advances linking molecular functions to biological outcomes. *Genes Dev* 31, 101–126. doi:10.1101/gad.291518.116 [PubMed: 28202539]
- Hengel SM, Goodlett DR, 2012 A Review of Tandem Mass Spectrometry Characterization of Adenosine Diphosphate-Ribosylated Peptides. *Int J Mass Spectrom* 312, 114–121. doi:10.1016/j.ijms.2011.06.003 [PubMed: 22563295]
- Hornung V, Hartmann R, Ablasser A, Hopfner K-P, 2014 OAS proteins and cGAS: unifying concepts in sensing and responding to cytosolic nucleic acids. *Nat Rev Immunol* 14, 521–528. doi:10.1038/nri3719 [PubMed: 25033909]
- Hottiger MO, 2015 Nuclear ADP-Ribosylation and Its Role in Chromatin Plasticity, Cell Differentiation, and Epigenetics. *Annu Rev Biochem*. doi:10.1146/annurev-biochem-060614-034506
- Hottiger MO, Hassa PO, Lüscher B, Schüler H, Koch-Nolte F, 2010 Toward a unified nomenclature for mammalian ADP-ribosyltransferases. *Trends Biochem Sci*. doi:10.1016/j.tibs.2009.12.003
- Ibsen MS, Gad HH, Thavachelvam K, Boesen T, Desprès P, Hartmann R, 2014 The 2'–5'-oligoadenylate synthetase 3 enzyme potently synthesizes the 2''–5''-oligoadenylates required for RNase L activation. *J Virol* 88, 14222–14231. doi:10.1128/JVI.01763-14 [PubMed: 25275129]
- James DI, Smith KM, Jordan AM, Fairweather EE, Griffiths LA, Hamilton NS, Hitchin JR, Hutton CP, Jones S, Kelly P, McGonagle AE, Small H, Stowell AIJ, Tucker J, Waddell ID, Waszkowycz B, Ogilvie DJ, 2016 First-in-Class Chemical Probes against Poly(ADP-ribose) Glycohydrolase (PARG) Inhibit DNA Repair with Differential Pharmacology to Olaparib. *ACS Chem. Biol* 11, 3179–3190. doi:10.1021/acschembio.6b00609 [PubMed: 27689388]
- Jewett JC, Bertozzi CR, 2010 Cu-free click cycloaddition reactions in chemical biology. *Chem Soc Rev* 39, 1272–1279. [PubMed: 20349533]
- Juarez-Salinas H, Sims JL, Jacobson MK, 1979 Poly(ADP-ribose) levels in carcinogen-treated cells. *Nature* 282, 740–741. [PubMed: 229416]
- Justesen J, Ferbus D, Thang MN, 1980 Elongation mechanism and substrate specificity of 2'', 5''-oligoadenylate synthetase. *Proc Natl Acad Sci USA* 77, 4618–4622. [PubMed: 6933509]
- Justesen J, Ferbus D, Thang MN, 1980 2'5' oligoadenylate synthetase, an interferon induced enzyme: direct assay methods for the products, 2'5' oligoadenylates and 2''5'' co-oligonucleotides. *Nucleic Acids Res* 8, 3073–3085. [PubMed: 6160465]
- Justesen J, Hartmann R, Kjeldgaard NO, 2000 Gene structure and function of the 2''–5''-oligoadenylate synthetase family. *Cell Mol Life Sci* 57, 1593–1612. [PubMed: 11092454]
- Kanai M, Miwa M, Kuchino Y, Sugimura T, 1982 Presence of branched portion in poly(adenosine diphosphate ribose) in vivo. *J Biol Chem* 257, 6217–6223. [PubMed: 7042708]
- Kawamitsu H, Hoshino H, Okada H, Miwa M, Momoi H, Sugimura T, 1984 Monoclonal antibodies to poly(adenosine diphosphate ribose) recognize different structures. *Biochemistry* 23, 3771–3777. [PubMed: 6206890]
- Keith G, Desgrès J, de Murcia G, 1990 Use of two-dimensional thin-layer chromatography for the components study of poly(adenosine diphosphate ribose). *Anal Biochem* 191, 309–313. [PubMed: 2085177]
- Kistemaker HAV, Nardoza AP, Overkleeft HS, van der Marel GA, Ladurner AG, Filippov DV, 2016 Synthesis and Macrodomein Binding of Mono-ADP-Ribosylated Peptides. *Angew. Chem. Int. Ed. Engl* 55, 10634–10638. doi:10.1002/anie.201604058 [PubMed: 27464500]
- Kleine H, Poreba E, Lesniewicz K, Hassa PO, Hottiger MO, Litchfield DW, Shilton BH, Lüscher B, 2008 Substrate-assisted catalysis by PARP10 limits its activity to mono-ADP-ribosylation. *Molecular Cell* 32, 57–69. doi:10.1016/j.molcel.2008.08.009 [PubMed: 18851833]

- Kristiansen H, Gad HH, Eskildsen-Larsen S, Desprès P, Hartmann R, 2011 The oligoadenylate synthetase family: an ancient protein family with multiple antiviral activities. *J. Interferon Cytokine Res* 31, 41–47. doi:10.1089/jir.2010.0107 [PubMed: 21142819]
- Krukenberg KA, Kim S, Tan ES, Maliga Z, Mitchison TJ, 2015 Extracellular Poly(ADP-Ribose) Is a Pro-inflammatory Signal for Macrophages. *Chem Biol* 22, 446–452. doi:10.1016/j.chembiol.2015.03.007 [PubMed: 25865309]
- Lambrecht MJ, Brichacek M, Barkauskaite E, Ariza A, Ahel I, Hergenrother PJ, 2015 Synthesis of Dimeric ADP-Ribose and its Structure with Human Poly(ADP-Ribose) Glycohydrolase. *J Am Chem Soc.* doi:10.1021/ja512528p
- Larsen SC, Hendriks IA, Lyon D, Jensen LJ, Nielsen ML, 2018 Systems-wide Analysis of Serine ADP-Ribosylation Reveals Widespread Occurrence and Site-Specific Overlap with Phosphorylation. *Cell Rep* 24, 2493–2505.e4. doi:10.1016/j.celrep.2018.07.083 [PubMed: 30157440]
- Leidecker O, Bonfiglio JJ, Colby T, Zhang Q, Atanassov I, Zaja R, Palazzo L, Stockum A, Ahel I, Matic I, 2016 Serine is a new target residue for endogenous ADP-ribosylation on histones. *Nat Chem Biol* 12, 998–1000. doi:10.1038/nchembio.2180 [PubMed: 27723750]
- Leslie Pedrioli DM, Leutert M, Bilan V, Nowak K, Gunasekera K, Ferrari E, Imhof R, Malmström L, Hottiger MO, 2018 Comprehensive ADP-ribosylome analysis identifies tyrosine as an ADP-ribose acceptor site. *EMBO Rep* 19, e45310. doi:10.15252/embr.201745310 [PubMed: 29954836]
- Leung AKL, 2014 Poly(ADP-ribose): An organizer of cellular architecture. *205*, 613–619. doi:10.1083/jcb.201402114
- Löhöfener J, Steinke N, Kay-Fedorov P, Baruch P, Nikulin A, Tishchenko S, Manstein DJ, Fedorov R, 2015 The Activation Mechanism of 2''–5''-Oligoadenylate Synthetase Gives New Insights Into OAS/cGAS Triggers of Innate Immunity. *Structure* 23, 851–862. doi:10.1016/j.str.2015.03.012 [PubMed: 25892109]
- Lord CJ, Ashworth A, 2017 PARP inhibitors: Synthetic lethality in the clinic. *Science* 355, 1152–1158. [PubMed: 28302823]
- Lüscher B, Bütepage M, Eckeil L, Krieg S, Verheugd P, Shilton BH, 2018 ADP-Ribosylation, a Multifaceted Posttranslational Modification Involved in the Control of Cell Physiology in Health and Disease. *Chem. Rev* 118, 1092–1136. doi:10.1021/acs.chemrev.7b00122 [PubMed: 29172462]
- Malanga M, Bachmann S, Panzeter PL, Zweifel B, Althaus FR, 1995 Poly(ADP-ribose) quantification at the femtomole level in mammalian cells. *Anal Biochem* 228, 245–251. doi:10.1006/abio.1995.1346 [PubMed: 8572302]
- Martello R, Leutert M, Jungmichel S, Bilan V, Larsen SC, Young C, Hottiger MO, Nielsen ML, 2016 Proteome-wide identification of the endogenous ADP-ribosylome of mammalian cells and tissue. *Nature Communications* 7, 12917. doi:10.1038/ncomms12917
- Martello R, Mangerich A, Sass S, Dedon PC, Bürkle A, 2013 Quantification of cellular poly(ADP-ribose) by stable isotope dilution mass spectrometry reveals tissue- and drug-dependent stress response dynamics. *ACS Chem. Biol* doi:10.1021/cb400170b
- McPherson RL, Abraham R, Sreekumar E, Ong S-E, Cheng S-J, Baxter VK, Kistemaker HAV, Filippov DV, Griffin DE, Leung AKL, 2017 ADP-ribosylhydrolase activity of Chikungunya virus macrodomain is critical for virus replication and virulence. *Proc Natl Acad Sci USA.* doi:10.1073/pnas.1621485114
- Min W, Bruhn C, Grigaravicius P, Zhou Z-W, Li F, Krüger A, Siddeek B, Greulich K-O, Popp O, Meisezahl C, Calkhoven CF, Bürkle A, Xu X, Wang Z-Q, 2013 Poly(ADP-ribose) binding to Chk1 at stalled replication forks is required for S-phase checkpoint activation. *Nature Communications* 4, 2993. doi:10.1038/ncomms3993
- Moulder L, Hedley ML, 2016 Tesaro Niraparib Pipeline Update (P014354) presented at the Annual Meeting of American Society of Clinical Oncology
- Moyle PM, Muir TW, 2010 Method for the synthesis of mono-ADP-ribose conjugated peptides. *J Am Chem Soc* 132, 15878–15880. doi:10.1021/ja1064312 [PubMed: 20968292]
- Palazzo L, Miko A, Ahel I, 2017 ADP-ribosylation: new facets of an ancient modification. *FEBS J.* doi:10.1111/febs.14078

- Palazzo L, Thomas B, Jemth A-S, Colby T, Leidecker O, Feijs K, Zaja R, Loseva O, Puigvert JC, Matic I, Helleday T, Ahel I, 2015 Processing of Protein ADP-ribosylation by Nudix Hydrolases. *Biochem J*. doi:10.1042/BJ20141554
- Pascal JM, Ellenberger T, 2015 The rise and fall of poly(ADP-ribose): An enzymatic perspective. *DNA Repair (Amst.)*. doi:10.1016/j.dnarep.2015.04.008
- Popp O, Veith S, Fahrer J, Bohr VA, Bürkle A, Mangerich A, 2013 Site-specific noncovalent interaction of the biopolymer poly(ADP-ribose) with the Werner syndrome protein regulates protein functions. *ACS Chem. Biol* 8, 179–188. doi:10.1021/cb300363g [PubMed: 23082994]
- Poulsen JB, Kjær KH, Justesen J, Martensen PM, 2015 Enzyme assays for synthesis and degradation of 2'-5As and other 2''-5'' oligonucleotides. *BMC Biochem*. 16, 15. doi:10.1186/s12858-015-0043-8 [PubMed: 26113370]
- Rouleau M, Patel A, Hendzel MJ, Kaufmann SH, Poirier GG, 2010 PARP inhibition: PARP1 and beyond. *Nat Rev Cancer* 10, 293–301. doi:10.1038/nrc2812 [PubMed: 20200537]
- Sarkar SN, Sen GC, 1998 Production, purification, and characterization of recombinant 2'', 5''-oligoadenylate synthetases. *Methods* 15, 233–242. doi:10.1006/meth.1998.0627 [PubMed: 9735308]
- Shah GM, Poirier D, Duchaine C, Brochu G, Desnoyers S, Lagueux J, Verreault A, Hoflack JC, Kirkland JB, Poirier GG, 1995 Methods for biochemical study of poly(ADP-ribose) metabolism in vitro and in vivo. *Anal Biochem* 227, 1–13. doi:10.1006/abio.1995.1245 [PubMed: 7668367]
- Slade D, Dunstan MS, Barkauskaite E, Weston R, Lafite P, Dixon N, Ahel M, Leys D, Ahel I, 2011 The structure and catalytic mechanism of a poly(ADP-ribose) glycohydrolase. *Nature*. doi: 10.1038/nature10404
- Tan ES, Krukenberg KA, Mitchison TJ, 2012 Large scale preparation and characterization of poly(ADP-ribose) and defined length polymers. *Anal Biochem*. doi:10.1016/j.ab.2012.06.015
- Vivelo CA, Wat R, Agrawal C, Tee HY, Leung AKL, 2016 ADPriboDB: The database of ADP-ribosylated proteins. *Nucleic Acids Res*. doi:10.1093/nar/gkw706
- Voorneveld J, Rack JGM, Ahel I, Overkleeft HS, van der Marel GA, Filippov DV, 2018 Synthetic α - and β -Ser-ADP-ribosylated Peptides Reveal α -Ser-ADPr as the Native Epimer. *Org. Lett* 20, 4140–4143. doi:10.1021/acs.orglett.8b01742 [PubMed: 29947522]
- Wang Z, Michaud GA, Cheng Z, Zhang Y, Hinds TR, Fan E, Cong F, Xu W, 2012 Recognition of the iso-ADP-ribose moiety in poly(ADP-ribose) by WWE domains suggests a general mechanism for poly(ADP-ribosyl)ation-dependent ubiquitination. *Genes Dev*. doi:10.1101/gad.182618.111
- Westcott NP, Fernandez JP, Molina H, Hang HC, 2017 Chemical proteomics reveals ADP-ribosylation of small GTPases during oxidative stress. *Nat Chem Biol* 13, 302–308. doi:10.1038/nchembio.2280 [PubMed: 28092360]
- Wienken CJ, Baaske P, Rothbauer U, Braun D, Duhr S, 2010 Protein-binding assays in biological liquids using microscale thermophoresis. *Nature Communications* 1, 100. doi:10.1038/ncomms1093
- Zhang F, Chen Y, Li M, Yu X, 2014 The oligonucleotide/oligosaccharide-binding fold motif is a poly(ADP-ribose)-binding domain that mediates DNA damage response. *Proc Natl Acad Sci USA* 111, 7278–7283. doi:10.1073/pnas.1318367111 [PubMed: 24799691]
- Zhang Y, Wang J, Ding M, Yu Y, 2013 Site-specific characterization of the Asp- and Glu-ADP-ribosylated proteome. *Nat Methods*. doi:10.1038/nmeth.2603
- Zhang Y, Liu S, Mickanin C, Feng Y, Charlat O, Michaud GA, Schirle M, Shi X, Hild M, Bauer A, Myer VE, Finan PM, Porter JA, Huang S-MA, Cong F, 2011 RNF146 is a poly(ADP-ribose)-directed E3 ligase that regulates axin degradation and Wnt signalling. *Nat Cell Biol* 13, 623–629. doi:10.1038/ncb2222 [PubMed: 21478859]
- Zhen Y, Yu Y, 2018 Proteomic Analysis of the Downstream Signaling Network of PARP1. *Biochemistry* 57, 429–440. doi:10.1021/acs.biochem.7b01022 [PubMed: 29327913]
- Zhen Y, Zhang Y, Yu Y, 2017 A Cell-Line-Specific Atlas of PARP-Mediated Protein Asp/Glu-ADP-Ribosylation in Breast Cancer. *Cell Rep* 21, 2326–2337. doi:10.1016/j.celrep.2017.10.106 [PubMed: 29166620]

HIGHLIGHTS

- ELTA labels free or protein-conjugated ADP-ribose monomers and polymers
- ELTA simplifies measurement of protein binding to PAR of a defined chain length
- ELTA enables assessment of PAR length from ADP-ribosylated proteins and cells
- ELTA allows enrichment of femtomole ADP-ribosylated peptides from complex mixtures

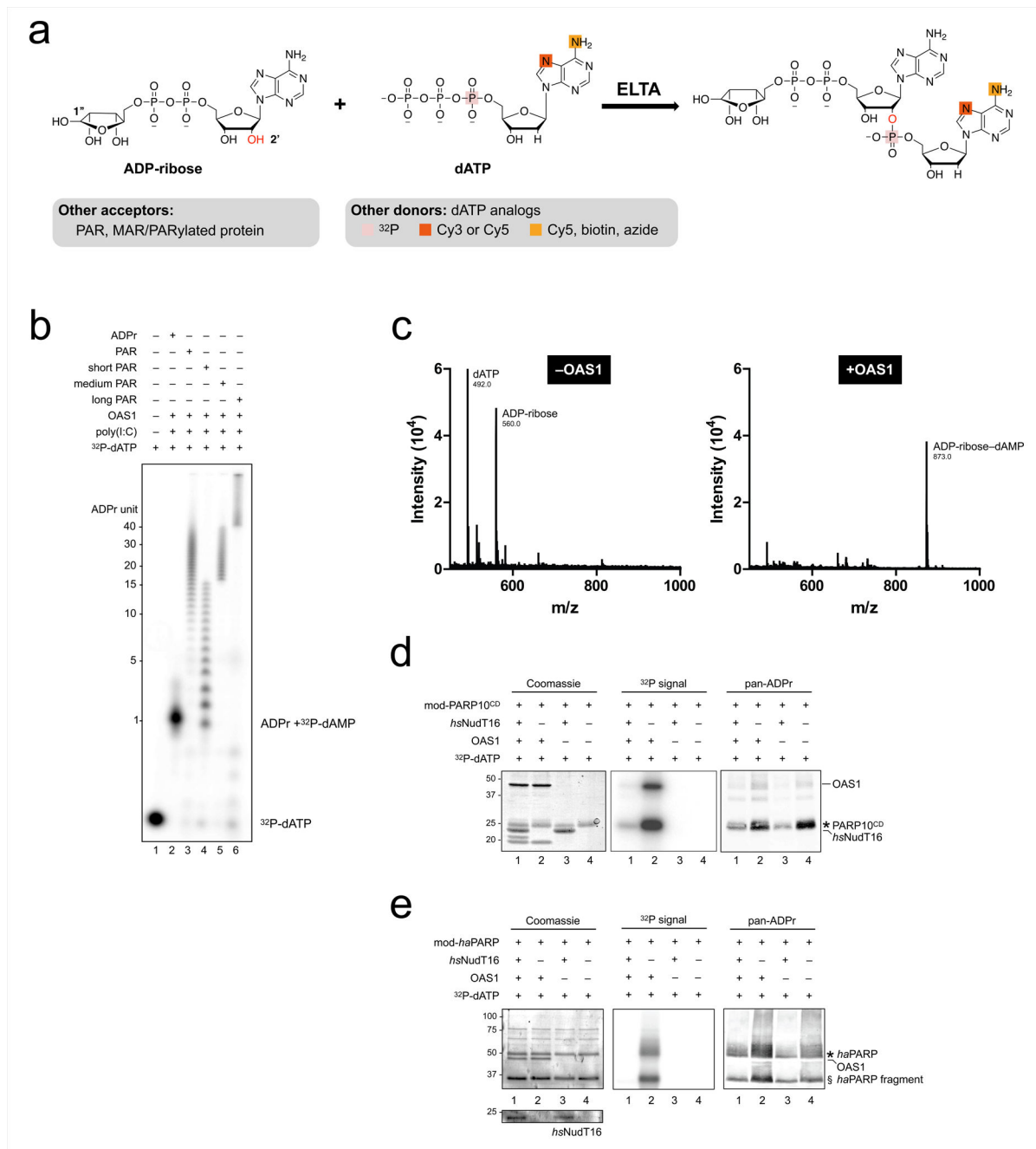


Figure 1. ELTA labels free or protein-conjugated ADP-ribose monomers and polymers.

(a) Schematics of ELTA. Free or protein-conjugated ADP-ribose can be labeled by incubating with OAS1 and dATP, where the 2'-OH terminus is indicated in red. Colored box indicates various dATP analogs that can also be used in the ELTA reactions, including radioactive (^{32}P), fluorescent (Cy3, Cy5), biotinylated or clickable analogs. (b) 15% urea-PAGE analyses of the addition of ^{32}P -dAMP onto ADP-ribose monomers and polymers using ELTA and visualized by autoradiograph. (c) MALDI-TOF analyses of the reaction of ADP-ribose with dATP, and with or without OAS1. (d-e) Analyses of the ELTA labeling reaction of (d) MARYlated PARP10 catalytic domain (mod-PARP10^{CD}) and (e) PARYlated

*ha*PARP (mod-*ha*PARP) using ^{32}P -dATP. Shown are a coomassie gel (left), an autoradiograph (middle), and a western blot probed with pan-ADP-ribose reagent (right). As negative controls, modified proteins were treated with the phosphodiesterase *hs*NudT16 to remove the 2'-OH termini of the ADP-ribose groups prior to ELTA labeling. For panel d, * indicates PARP10; OAS1 was ADP-ribosylated by PARP10 with the remnant of NAD^+ , and, therefore, detected by pan-ADP-ribose reagent and labeled by OAS1. For panel e, * indicates *ha*PARP and § indicates *ha*PARP fragments that were also ADP-ribosylated and, therefore, detected by pan-ADP-ribose reagent and labeled by OAS1.

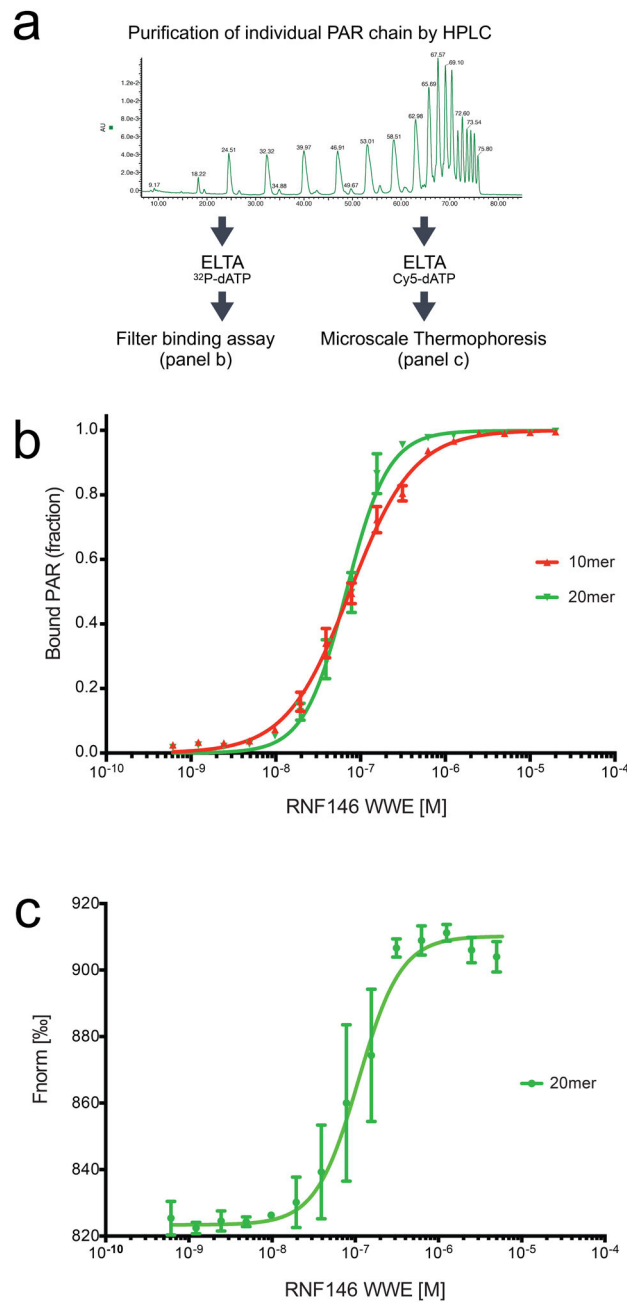


Figure 2. Biophysical measurement of interaction between PAR-binding protein domain WWE and PAR of defined chain length.

(a) Workflow used for ELTA-modified PAR of defined length for biophysical measurement. The details of HPLC run are illustrated in Fig. S1c. (b) Filter binding assay of RNF146 WWE domain binding to 10- and 20-mer PAR, which were radiolabeled using ELTA and ^{32}P -dATP. (c) MST analysis of RNF146 WWE domain binding to 20-mer PAR, which was labeled using ELTA and Cy5-dATP.

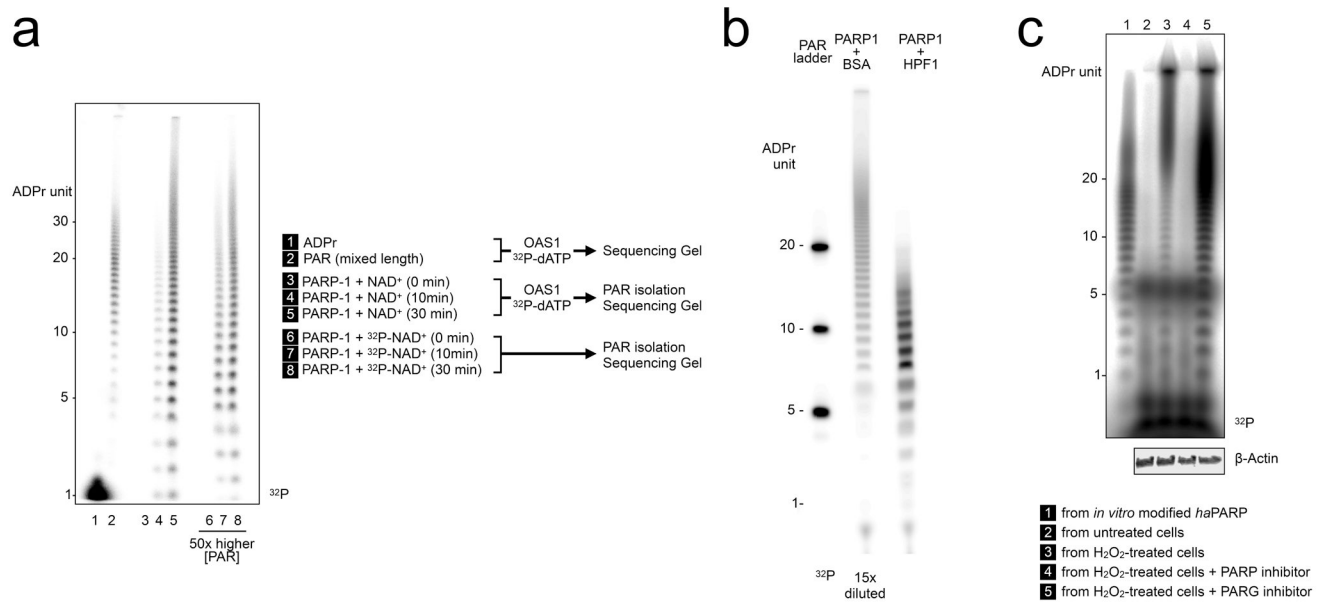


Figure 3. Detection of ADP-ribose length from individual proteins and cells using ELTA.

(a) 15% urea-PAGE analyses of the ELTA labeling reaction of ADP-ribose monomer (lane 1) and PAR of mixed length (lane 2), as well as ADP-ribose monomers and polymers isolated from PARP1 automodification reactions with 1 mM NAD⁺ for 0 (lane 3), 10 (lane 4), or 30 min (lane 5) that were labeled by OAS1 and ³²P-dATP. As a comparison, the ADP-ribose isolated from PARP1 automodification reaction in the same time frame with 1 mM NAD⁺ with a trace of ³²P-NAD⁺ were loaded in lanes 6–8. We note that 50-fold less of the reaction were loaded in lanes 3–5 compared with lanes 6–8. (b) 15% urea-PAGE analyses of ELTA labeling reaction of ADP-ribose monomers and polymers isolated from automodification of PARP1 along with either BSA and HPF1. The first lane contained ELTA-labeling of an equal mole of 5-, 10- and 20-mer PAR. The reaction in the PARP1+BSA lane was diluted 15 times in water prior to ELTA labeling. (c) 15% urea-PAGE analyses of the ELTA labeling reaction of ADP-ribose isolated from *in vitro* modified haPARP (lane 1), from untreated HaCaT cells (lane 2), from HaCaT cells treated with 1 mM H₂O₂ for 10 min (lane 3), from HaCaT cells treated with 1 mM H₂O₂ for 10 min, but pre-treated the cells with 20 μM PARP inhibitor Olaparib for 2 h (lane 4), or pre-treated with 1 μM PARG inhibitor PDD00017273 for 2 h (lane 5). Corresponding lysates of cells from lanes 2–5 were probed with β-actin.

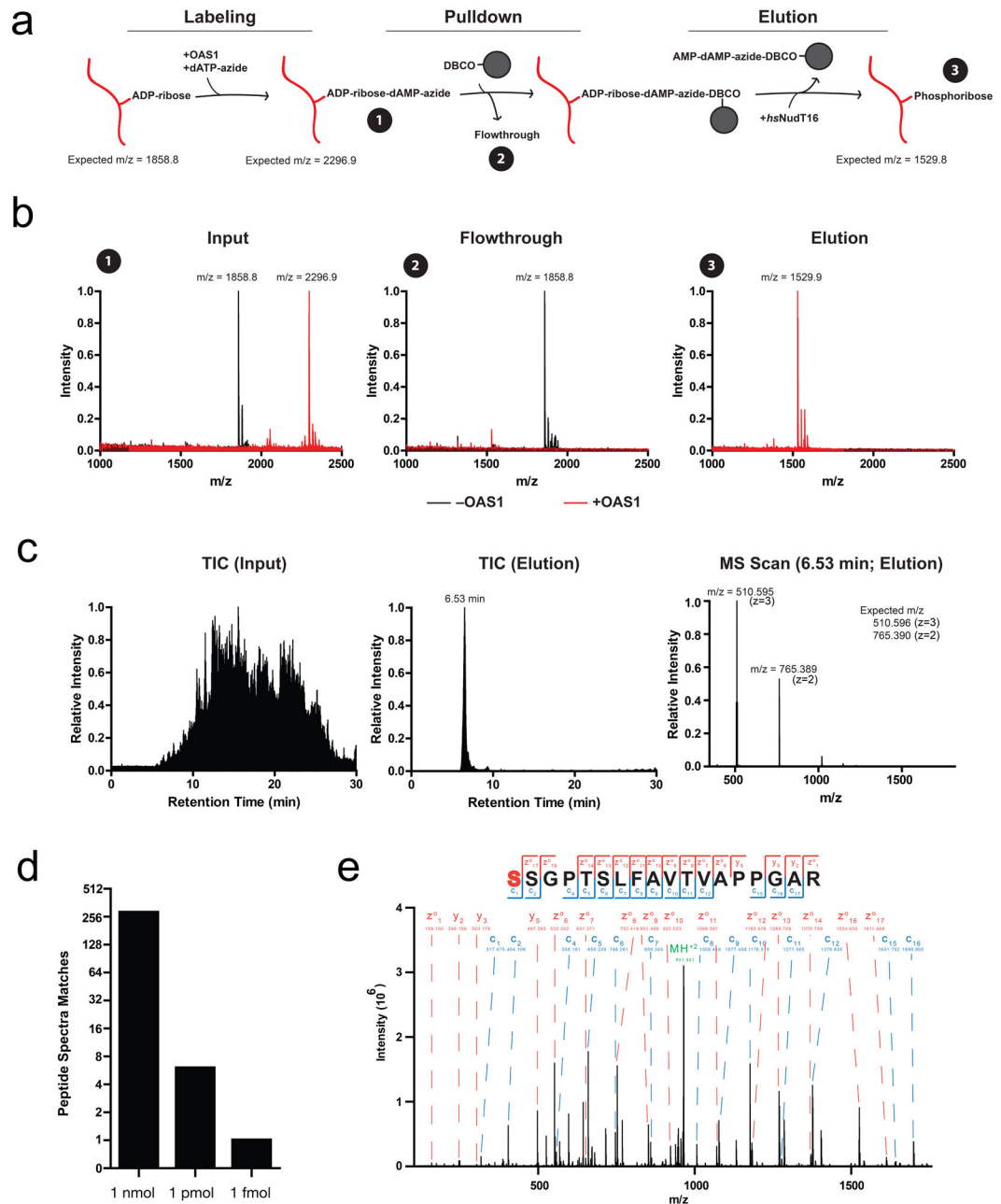


Figure 4. Enrichment of ELTA-labeled ADP-ribosylated peptides from complex mixtures.

(a) Schematics of the pipeline to selectively label and enrich ADP-ribosylated peptides. (b) MALDI-TOF analyses of (1) the reaction mixtures after ELTA but prior to enrichment, (2) the flowthrough from the enrichment matrix, (3) the eluant with the phosphodiesterase *hsNudT16*. The m/z traces shown are the overlay of two experiments, where red lines indicate samples with OAS1 and black lines indicate samples without OAS1. (c) The total intensity chromatograph (TIC) of the input sample (left), which includes 1 nmol of ADP-ribosylated peptide HK533 in 1 mg cell lysate peptides, and of the enriched sample after elution (middle) and the mass spectrometry scan analyses at the retention time of 6.53 min

(right). (d) Quantification of the peptide-spectrum matches (PSM) to the ADP-ribosylated peptide HK533 enriched from 1 mg cell lysate peptides, which are dosed with either 1 nmol, 1 pmol, or 1 fmol HK533. (e) Identified MS/MS spectra of a tryptic peptide identified from endogenous hnRNPU, with the modification site signified by the addition of a phosphoribose group (red).

Key Resources Table

REAGENT or RESOURCE	SOURCE	IDENTIFIER
Antibodies		
Rabbit polyclonal anti-PAR	Trevigen	Cat#4336-BPC-100
Anti- β -actin(CloneAC15)	Millipore Sigma	RRID: AB_476692
pan-ADP-ribose binding reagent	Millipore	Cat#MABE1016; RRID: AB_2665466
IRDye 800CW Streptavidin	VWR	Cat#RLS000-31
Bacterial and Virus Strains		
<i>E. coli</i> BL21 codon plus (DE3)-RIPL	Agilent Technologies	Cat#130280
<i>E. coli</i> RosettaDE3	In-house	
Chemicals, Peptides, and Recombinant Proteins		
α - ³² P-dATP	Perkin Elmer	Cat#NEG512H250 UC
Cy3-dATP	Perkin Elmer	Cat#NEL592001 EA
Cy5-dATP	Perkin Elmer	Cat#NEL593001EA
N ⁶ -(6-amino)hexyl-dATP-Cy5	Jena Bioscience	Cat#NU-835-CY5
N ⁶ -(6-Azido)hexyl-dATP	Jena Bioscience	Cat#CLK-NU-002
Biotin-14-dATP	ThermoFisher	Cat#19524016
DBCO-agarose	Click Chemistry Tools	Cat#1034
StrepTactin resin	IBA Life Sciences	Cat#2-1201-025
OAS1	This paper	N/A
PARP1	Langelier et al. 2011	N/A
HPF1	Gibbs-Seymour et al. 2016	N/A
PARP10 catalytic domain (PARP10 ^{CD})	McPherson et al., 2017	N/A
haPARP	Slade et al., 2011	N/A
hsNudT16	Daniels et al., 2015	N/A
HK533	Kistemaker et al., 2016	N/A
JV099	Voorneveld et al., 2018	N/A
Activated DNA	Trevigen	Cat#4671-096-06
Low molecular weight poly(I:C)	Invivogen	Cat#tlrl-picw
RNaseA	ThermoFisher	Cat#EN0531
DNaseI	Roche	Cat#10104159001
Proteinase K (as part of High Pure miRNA Isolation Kit)	Roche	Cat#05080576001
Lysyl Endopeptidase	Wako Chemicals	Cat#129-02543
Trypsin Protease, MS Grade	ThermoFisher	Cat#90058
Sigmafast Protease Inhibitor Tablets	Millipore Sigma	Cat#S8830
TCEP	Life Technologies	Cat#T2556

REAGENT or RESOURCE	SOURCE	IDENTIFIER
CAM	Fisher Scientific	Cat#AC14841-0050
2,5-dihydroxybenzoic acid	Millipore Sigma	Cat#149357
β -Nicotinamide adenine dinucleotide sodium salt (NAD ⁺)	Millipore Sigma	Cat#N0632
Adenosine 5'-diphosphoribose sodium salt	Millipore Sigma	Cat#A0752
SYBR Gold	Invitrogen (ThermoFisher)	Cat#S11494
Hydrogen peroxide solution (H ₂ O ₂)	Millipore Sigma	Cat#H1009
Olaparib	Selleckchem	Cat#S1060
PDD 00017273	Tocris	Cat#5952
Critical Commercial Assays		
High Pure miRNA Isolation Kit	Roche	Cat#05080576001
RiboZol Plus RNA purification kit	VWR	Cat#97064-954
Pierce™ color silver stain kit	ThermoFisher	Cat#24597
Deposited Data		
Mass Spectrometry data	MassIVE	MSV000083141
Experimental Models: Cell Lines		
HeLa	ATCC	Cat#CCL-2
Spodoptera frugiperda (SF9) cells	ThermoFisher	Cat#114496015
BL-21 codon plus (DE3)-RIPL	Agilent Technologies	Cat#130280
HaCaT	Coulombe's lab (BMB,SPH, Johns Hopkins)	RRID: CVCL_0038
Oligonucleotides		
5' GGGTTGCGCCGCTTGGG 3'	Langelier et al 2011	
3' CCCAACGCCGCGAACCC 5'	Langelier et al 2011	
Recombinant DNA		
pFI Strep Sumo TEV OAS1	This paper	N/A
pET28a His Sumo TEV RNF146 WWE domain	This Paper	N/A
Software and Algorithms		
GeneTools software	Synoptics	
MaxQuant version 1.5.7.4	N/A	http://www.coxdocs.org/doku.php?id=maxquant:start
Prism 6	GraphPad	https://www.graphpad.com/scientific-software/prism/
MO.Affinity analysis	NanoTemper	https://nanotempertech.com/monolith/
GeneTools	Synoptics	https://www.syngene.com/software/genetools-automatic-image-analysis/
ImageStudio 5.2.5	Li-Cor	https://www.licor.com/bio/products/software/image_studio/
Other		

REAGENT or RESOURCE	SOURCE	IDENTIFIER
Bench protocol	This paper	Methods S1
Monolith NT.115 Pico	NanoTemper	https://nanotempertech.com/monolith/

Author Manuscript

Author Manuscript

Author Manuscript

Author Manuscript